Seismic Re-assessment of the Leaning Tower of Pisa: Dynamic Monitoring, Site Response & SSI

Gabriele Fiorentino,[a)] M.EERI, Giuseppe Quaranta,[b)] George Mylonakis, [e)f)g)] M.EERI, Davide Lavorato,[a)] Alessandro Pagliaroli,[c)] Giorgia Carlucci,[d)] Fabio Sabetta,[h)] Giuseppe Della Monica,[d)] Giuseppe Lanzo,[b)] Victoria Aprile,[c)] Giuseppe Carlo Marano,[h) i)] Bruno Briseghella,[h)] Giorgio Monti,[b)j)] Nunziante Squeglia,[k)] Raffaello Bartelletti, [k)] and Camillo Nuti, [a)h)l)] M.EERI

The Tower of Pisa survived several strong earthquakes over the last 650 years - despite its leaning and limited strength & ductility. No credible explanation for its remarkable seismic performance exists to date. A re-assessment of this unique case history in light of new seismological, geological, structural and geotechnical information is reported, aiming to address the above question. The following topics are discussed: (1) dynamic structural identification based on recorded earthquake data; (2) geophysical site characterization using a 2D array; (3) seismic hazard and site response analysis considering horizontal and vertical motions; (4) soil-structure interaction analysis calibrated using lab and field data. A substantial shift in natural period, from about 0.35s to over 1s (a threefold increase – the largest known for a building of that height) due to SSI, a wave parameter ($1/\sigma$) of about 0.3, and a minor effect of vertical ground motion are identified, and may explain the lack of

a) Department of Architecture, Roma Tre University, Italy
b) Department of Structural and Geotechnical Engineering, Sapienza University of Rome, Italy
c) Department of Engineering and Geology, University of Chieti – Pescara, Italy
d) Department of Science, Roma Tre University, Via della Vasca Navale 84, Rome 00146, Italy
e) Department. of Civil Engineering, University of Bristol, UK
f) Department of Civil Engineering, University of Patras, Greece
g) Department of Civil and Environmental Engineering, University of California at Los Angeles, U.S.A.
h) College of Civil Engineering, Fuzhou University, China
i) Department of Science of Civil Engineering and Architecture, Technical University of Bari, Italy
j) College of Civil Engineering, Nanjing Tech University, China
k) Department of Civil and Industrial Engineering, University of Pisa, Italy
l) Corresponding Author

earthquake damage on the Tower. Recommendations for future research, including the need to establish a seismic bedrock deeper than 500m, are provided.

INTRODUCTION

Motivations and layout of the present paper

Preservation of architectural heritage is an important matter in modern societies, which has attracted significant research attention in recent times. The conservation of the built heritage contributes, on one hand, towards consolidating collective memory and cultural identity while, on the other hand, plays a role in strengthening the local economy in different ways including tourism, education and lifestyle. The high seismicity and the exceptional concentration of vulnerable historical buildings makes the Italian architectural heritage stock exposed to high risks. Recent Italian earthquakes – such as those in L'Aquila (2009), Reggio Emilia (2012) and Central Italy (2016) – have demonstrated the susceptibility of historical buildings to strong ground shaking, especially at close distances from source.

Within this framework, the herein reported research is concerned with the seismic behavior of the Leaning Tower of Pisa, the structural assessment of which is of great scientific and engineering interest. Several studies of this unique monument have been carried out in the last decades, and are mainly associated with the causes and consequences of its quasi-static movements due to leaning instability (Burland et al. 2013). Based on these studies, successful geotechnical interventions have been carried out to reverse the leaning (Burland et al. 2009). On the other hand, investigations of seismic actions, including dynamic soil-structure interaction and the dynamic behavior of the structure, have received less attention. The multi-disciplinary research group co-authoring this article was assembled and started working in 2014 to produce original data for supporting new studies on the seismic vulnerability assessment of the Tower.

The paper at hand is the first comprehensive report put together by this group, though a few preliminary reports (e.g. Fiorentino et al. 2017, 2018) have provided some highlights. Following a review of the relevant literature, including construction history (Macchi and Ghelfi 2002), the following issues are discussed: (i) dynamic monitoring and identification based on recent earthquake recordings using up-to-date techniques, (ii) an enhanced subsoil model developed by geophysical means using an extended two-dimensional geophysical array, (iii) definition of the expected earthquake input through pertinent hazard analysis using both

probabilistic and deterministic approaches, iv) site response analysis considering both horizontal and vertical ground motion components, (v) development of a simplified elasto-dynamic model of the tower encompassing soil-structure interaction via pertinent foundation springs, calibrated using geotechnical data and optimization tools, (vi) earthquake response of the tower using response spectrum and time history analysis. Each issue is discussed in detail in the ensuing.

Review of history of construction works and interventions

The Leaning Bell Tower, the Cathedral of Santa Maria Assunta, the Monumental Cemetery and the Baptistery are famous religious structures located in Piazza del Duomo (also known as Piazza dei Miracoli) in Pisa. They four monumental structures have been included in the list of World Heritage Sites by UNESCO since 1987. The Leaning Tower was built in a period spanning three centuries. Its construction began in 1173 and was suspended in 1178, due to war, when the erection of the fourth level (Ordine) was still in progress. Construction was resumed in 1272 and interrupted again in 1278. In 1370 it was finally completed with the erection of the belfry. New floors were taller on one side to reduce eccentricity. The final inclination was 1.6°, corresponding to an offset of 1.6 m at the top (about 1/3 of the present value). The history of construction is depicted in Figure 1a and has been discussed in literature (e.g. Squeglia & Bentivoglio 2015).

The so called Catino (i.e. *basin,* Figure 1b, 1c) was built in 1838-1839, after unveiling the basement of the Tower. With the intention to enlarging and stabilizing the foundation of the monument, the ring-shaped space was filled with rock blocks cemented with lime.

The Department of Civil Works of the Town of Pisa carried out some interventions in the period 1933-1935 concerning the waterproofing and the consolidation of the foundation plinth with injections of cement grout. Moreover, the floor and walls of the Catino were protected by an 80 cm thick concrete slab, covered with marble. Studies carried out in the period 1993-1994 demonstrated that the inclination of the Tower continued to increase with time (had reached 5.5° in 1993), partly because of the seasonal variation in elevation of the water table located a few meters below ground level. In 1993, the Committee for the safeguard of the Pisa Tower (to be referred hereafter to as *the Committee*) approved temporary stabilization measures by posing 600 t of lead weights (installed in 1993 and increased to 900 t in 1995), acting as counterweight on the up-lifted North side of the foundation. The Tower was also secured with

two stabilizing cables anchored to two steel structures placed behind the building housing the offices of the Owner of the Tower (Opera della Primaziale Pisana, Figure 1c).

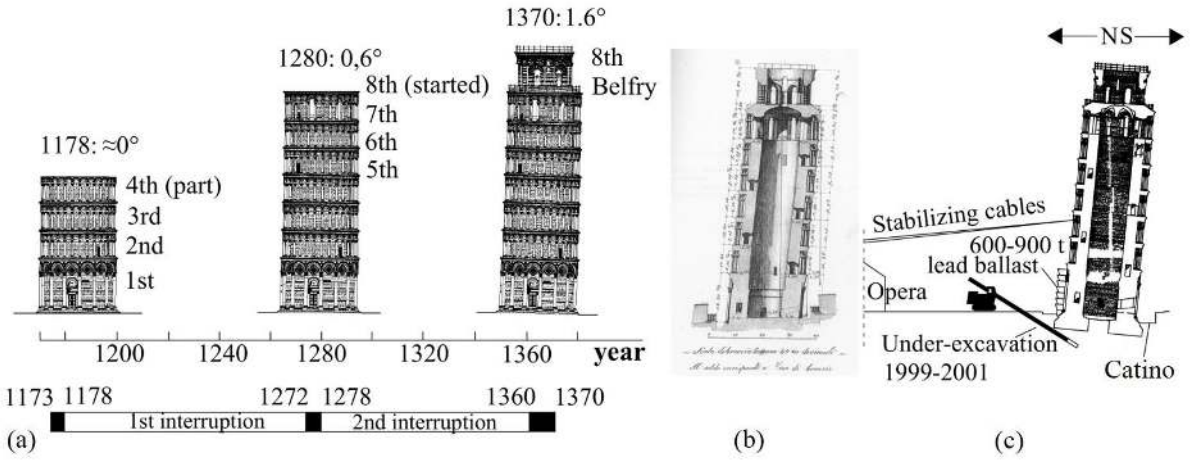

Figure 1. (a) History of the construction of the Tower (modified from Squeglia & Bentivoglio 2015), (b) Tower configuration as surveyed on 1817 (Cresy et al., 1829), (c) Temporary stabilization system, 1993-2001 (modified from Burland et al. 2013) with indication of the Catino (basin) created around the foundation.

After a large-scale test on a 7-m diameter circular foundation model and several numerical studies (Burland et al. 2013), the Committee approved under-excavation works alongside the Tower. A preliminary soil extraction was made between February and October 1999 within a 6-m wide zone. The main under-excavation began in December 1999 and continued through multiple steps until June 2001, when the stabilizing cables were removed. The soil extraction resulted in a reduction in tilt by about 10% (0.54°) which brought the leaning back to the levels experienced in the 1800's (Squeglia and Bentivoglio, 2015).

Meanwhile, the concrete slab at the base of the Catino was rigidly connected to the foundation of the Tower using inox steel rebars reinforced by post-tensioned cables (Figure 2). In addition, a drainage system was installed on 2002 to control the oscillations of the groundwater level, whose fluctuations are linked to the gradual increase in tilting.

Tower geometry and material properties

The Tower has a total height of 58.4 m measured from the base (56 m from ground level). The diameter of the superstructure is about 17 m including the external lodges (Figure 3a) and about 12 m without the lodges. The diameter of the central opening ranges from 7.3 m to 7.7 m. The foundation of the Tower has a ring shape with an external diameter of 19.6 m.

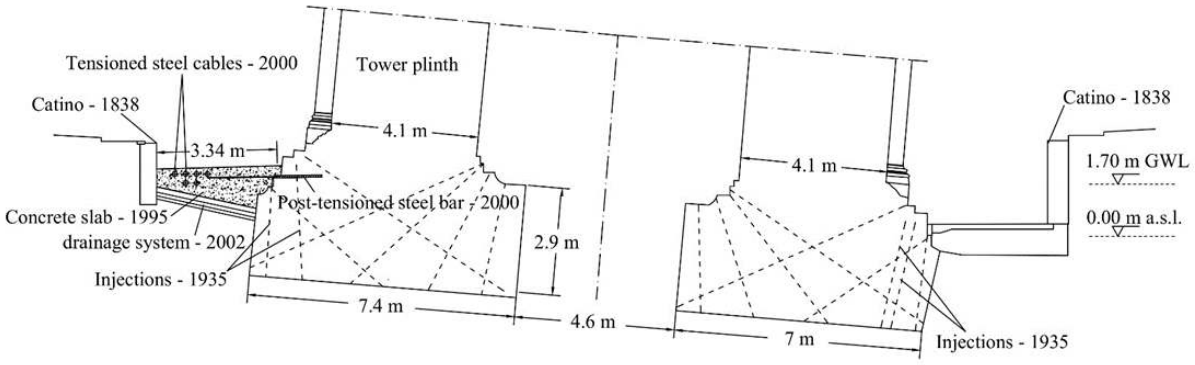

Figure 2. Foundation and Catino, GWL = Ground Water Level. (modified from Consorzio Progetto Torre di Pisa, 2000).

The thickness of the ring in horizontal plane is approximately 7.4 m and its embedment is about 2.9 m. The internal diameter of the foundation is 4.5 m leading to a contact area with the soil of about 285 m^2. The foundation rests on a masonry layer that was subjected to interventions of waterproofing concluded in 1935. The uncertainty in the values of the material parameters of the Tower was reduced following a number of studies conducted as part the activities of the Committee in the 1990's. Several non-destructive tests were undertaken to evaluate more accurately the characteristics of the outer and the inner walls (S. Giuliano Marble), of the rubble stone masonry, and the variation of the parameters with height. The Tower has an estimated weight of approximately 145,000 kN, leading to an average contact pressure due to gravity of about 510 kPa. The height of the center of mass from the base foundation is 22.6 m (Grandori & Faccioli 1993; Macchi & Ghelfi 2005). The tilt of the Tower is currently (2018) about 5° along the North-South direction (leading to an overhang of 5 m), whereas a minor tilt also exists in the East-West direction. Figure 3a depicts a side view in North-South direction and a cross-section of the Tower. A detail of the foundation is shown in Figure 3b.

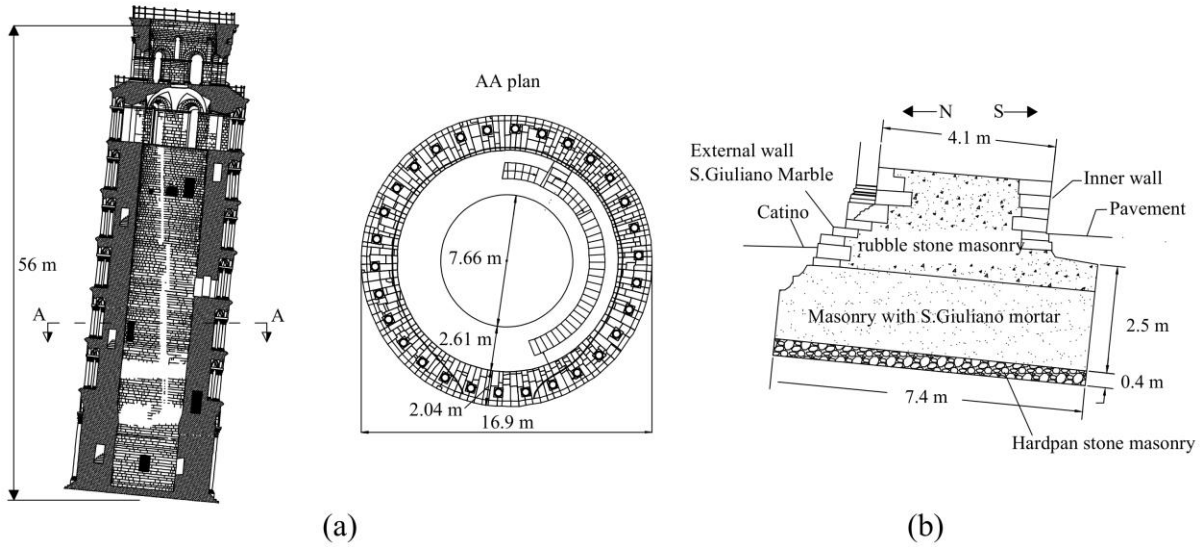

Figure 3. (a) Side view of the Tower in North-South direction and cross-section at the third level (right) – , (b) Detail of the foundation of the Tower (modified from Alisud 1996).

Previous dynamic measurements

Several experimental studies were carried out in recent times to estimate the dynamic characteristics of the Tower. One of the earliest investigations is the one by Nakamura et al. (1999). In that study, the authors installed two tri-axial sensors on the ground floor to record microtremors. Two sensors were also installed on each floor in a sequence. The temporary stabilization works were still in progress at the time, and the dynamic recordings were conducted when lead blocks were applied at the base of the Tower. A dynamic monitoring under vibrations induced by a vibrodyne was performed in January 1995 (Macchi and Ghelfi 2005). The sensor network consisted of Geotech-Teledyne model S13 seismometers placed at each level of the Tower. Atzeni et al. (2010) performed a remote survey by interferometric sensing in July 2008. In that case, the dynamic response was acquired with people inside the structure and a moderate wind intensity associated with a speed of about 5 m/s. More recently, Castellaro and Mulargia (2010) monitored the response at nine vertically-aligned measurement points on the Tower by means of velocimetric instruments (Tromino tromographs) on March 31st, 2009, when the structure was closed to tourists due to strong wind. Nowadays the Tower is equipped with a continuous dynamic monitoring system installed in 2002 (Macchi and Ghelfi 2005).

Previous soil investigations at the site

The soil underlying Piazza del Duomo has been studied by many authors (Cestelli Guidi et al. 1971; Desideri et al. 1997; Rampello and Callisto 1998; Burland et al. 2013). The subsoil

is composed of recent deposits dating back to the Pleistocene-Holocene having tidal origin. There are silts, clays and fine sands present, with intercalation of Aeolian sands from ancient coastal dunes.

The ground beneath the Tower consists of three principal geological formations, which are defined in the following (Cestelli Guidi et al. 1971).

- Layer A of approximately 10 m thickness, composed of soft estuarine deposits of sandy and clayey silts laid down under tidal conditions.
- Layer B made of soft sensitive normally consolidated marine clay, extending to a depth of about 40 m. Within this layer, it is possible to identify:
  - upper clays (Pancone) extending from 10 m to 21 m. They are characterized by low to medium consistency encompassing lightly over-consolidated and normally-consolidated clays,
  - intermediate clays whose depth ranges from 21 m to 25 m. They are over-consolidated clays characterized by high consistency,
  - intermediate sands, whose depth ranges from 25 m to 27 m,
  - lower clays, extending from 27 m to 40 m. They are normally-consolidated clays with medium to high consistency,
- Layer C made of dense marine sand that reaches a depth of about 60 m.

Layer A lies on a quasi-horizontal plane close to the foundation, except for a depression under the Tower where the weight of the superstructure has caused a settlement of about 2 m. Several geophysical tests have been performed to determine the shear wave velocity profile with depth (V_s). These include Down Hole tests (DH) conducted in 1993 (Grandori and Faccioli 1993), Cross Hole tests (CH) dating back to 2000 (Consorzio Progetto Torre di Pisa, 2000), DH and CH tests completed in 2005 (Viggiani and Pepe 2005), all performed in the vicinity of the Tower, and a SMDT test carried out in 2015 close to the Baptistry (Opera della Primaziale Pisana 2015). The results obtained from these tests show a satisfactory agreement of the measured V_s values. All the tests reached a maximum depth of 40 m except for the CH test conducted in 2000, which reached a depth of 65 meters. None of the tests was successful in identifying a "seismic bedrock" associated with a shear wave velocity in excess of 800 m/s.

Previous studies of seismic input

In their pioneering study, Grandori and Faccioli (1993) identified relevant seismic events between years 1087 and 1984. The maximum intensity in the Modified Mercalli scale (I_{MCS}) in Pisa was deemed higher than V (moderate). Specifically, it was pointed out that an I_{MCS} of VI occurred four times within a time window of 700 years (1280-1980) without inflicting damages to the Tower. Based on standard correlations between MCS intensity and PGA (Margottini et al. 1992) an intensity VI corresponds roughly to a PGA of 0.07g, while an intensity VII corresponds to a PGA of 0.12g. A seismic hazard analysis performed by Grandori and Faccioli indicated return periods T_R of 130 and 500 years for these values of PGA, respectively. The above authors argued that a 500-year seismic event could result in considerable risk for the Tower, although they did not evaluate the corresponding seismic input. Grandori & Faccioli also defined a horizontal response spectrum to be used as seismic input for dynamic analyses. The spectrum was obtained by enveloping the horizontal response spectra of actual recorded accelerograms extracted from a database of Italian earthquakes available at the time (Postpischl et al. 1991). The selection of the accelerograms was performed by considering magnitudes between 5.4 and 6.8, distances from source between 24 and 53 km and the geotechnical/geological conditions of the site. The horizontal components of eight accelerograms were selected and each record was scaled to a PGA of 0.07g. The median value and standard deviation were evaluated as well. The horizontal spectrum for the dynamic analyses was defined as the median value plus one standard deviation. Also, a vertical response spectrum was defined by scaling the vertical components to a PGA of 0.037g. The definition of the seismic input was re-examined by the same authors (Grandori et al. 1999). In their second study, they evaluated 20 synthetic accelerograms based on a hybrid deterministic-stochastic method (Ordaz et al. 1995) which included simulation of the 1920 Garfagnana earthquake, and came up with a similar response spectrum to that proposed in 1993.

Previous dynamic modelling of the Tower including soil-structure interaction

The first study encompassing soil-structure interaction was the one by Grandori and Faccioli (1993) and involved two different models for the soil. The first one was a homogeneous half-space, whereas the second considered a homogeneous surface layer on rigid rock. The two approaches led to similar results, and thus the dynamic impedances based on the half-space assumption were calculated through the theory of ring-shaped footings developed by Veletsos and Wei (1971). The Tower was modelled by means of a stick-type finite element

model. Neither the inclination of the structure nor the Catino were modelled. The fundamental period of the Tower obtained in that work was about 30% longer than the one established from recent experimental studies, a deviation which can be attributed to the use of a low value for the soil shear modulus corresponding to ~~account for~~ far-field conditions and accounting for modulus degradation during strong shaking. An evaluation of the effects of soil-structure interaction was also undertaken by Istituto Sperimentale Modelli e Strutture (1992). In that case, three stick-type finite element models were employed. The most accurate one was established by calibrating the stiffness of the springs at the base (without considering vertical oscillations) and the elastic moduli of the materials of the Tower, to fit the results of the experimental modal analysis.

SEISMIC MONITORING

Sensor network

The Tower is currently equipped with a permanent sensor network designed for seismic monitoring that consists of uniaxial accelerometers EpiSensor FBA ES-U and tri-axial accelerometers EpiSensor FBA ES-T. Their main characteristics are listed in Figure 4b.

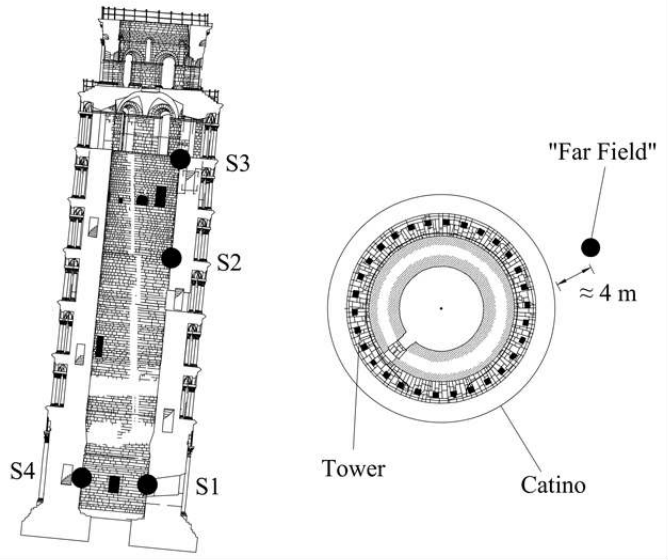

(a)

Parameter	Value
Sensor type	Force-balance
No. of axes	1 or 3
Full-scale range	± 0.25g
Sensitivity	10 V/g
Bandwidth	DC to 200 Hz
LP and HP filter	100 Hz-0.08 Hz
Dynamic range	About 90 dB
Resolution	16 bit
Sampling frequency	400 Hz

(b)

Figure 4. (a) Positions of the accelerometers on the Tower and on the ground, (b) Main characteristics of seismic sensor network.

Four measurement points have been selected on the Tower (Figure 4a). Points S1 (1st level), S2 (4th cornice) and S3 (6th cornice) have been equipped with tri-axial accelerometers with

their axes oriented East-West, North-South[1] and Vertical. An uniaxial accelerometer has been also installed at measurement point S4 (1st level), oriented along the vertical direction.

In addition to the sensors installed on the Tower, the dynamic monitoring network encompasses a tri-axial accelerometer installed on the ground surface (Figure 4a), which is intended for free-field recordings. As its location is very close to the foundation, however, the recordings might be affected by structural response. This sensor is out of order since 2012. The dynamic response of the Tower is recorded using a cyclic buffer with pre-defined length and user-defined triggering threshold. The specifications of the array are shown in Figure 4b.

Experimental seismic response of the Tower

Since the installation of the existing sensor network, only a limited number of earthquakes have triggered the vertical array. Table 1 presents the frequencies of the fundamental mode along the two directions for all selected seismic events, together with the corresponding groundwater level. These results suggest that the natural frequency of the fundamental mode does not change significantly for the minor levels of peak ground accelerations (between 1 and 5 gal) and variations of ground water table elevation (up to 0.25 m). For all recorded seismic events, the natural frequency along the North-South direction is slightly smaller than the one identified along the East-West direction.

Analysis of the recordings was possible for the six seismic events listed in Table 1, which date from 2004 to 2015. The table reports, for each event, the moment magnitude M and the epicentral distance from the site R, together with the maximum acceleration recorded on the Tower and the far field. It can be observed that the maximum recorded structural acceleration (at point S3) is rather low, about 8 gal.

The last earthquake of a moment magnitude greater than 5 for which seismic recordings are available occurred in 2012 (27/01/2012 Emilia event).

The fixed-base motion was established for sensor S3 by applying the following standard procedure (Sun, H. and Büyüköztürk, 2018):

$$V = \left(S_4^{(v)} + S_1^{(v)}\right)/2 \tag{1}$$

[1] The exact orientation coincides with the direction of maximum inclination (about 2 degrees from NS).

$$\theta = \left(S_4^{(v)} - S_1^{(v)}\right)/L \tag{2}$$

$$S_3^{(str)} = S_3^{(h)} - S_1^{(h)} - \theta\,\Delta H \tag{3}$$

where V = V(t) is the vertical acceleration at the base of the Tower, θ is the corresponding rotational acceleration, ΔH is the difference in elevation between stations S1 and S3 (about 36.4 m), and L is the horizontal distance between stations S1 and S4 (about 7.3 m).

The overall flexible-base motion (N-S component of original record at locations S3) and the fixed-base motion obtained by Equation 3 were analysed using the Continuous Wavelet Transform (CWT) for the 27/01/2012 Emilia event, as depicted in Figure 5. The interested reader can refer to Kramer et al. (2015) and Karimi et al. (2017) for alternative time-frequency analysis methods. Alternative identification techniques applicable to SSI-related problems are summarized in Star et al (2018).

Table 1. Seismic events (N = North-South, E = East-West); PTA (= Peak Tower Acceleration) ~~is~~ recorded in S3 and PGA (= Peak Ground Acceleration) by the far-field instrument; Natural frequency of the Tower along N and E directions, and corresponding groundwater levels. ONF = Observed Fundamental Natural Frequency; GWL = Ground Water Level.

Event	Date (dd/mm/yyyy)	M_W	R [km]	PGA [gal]		PTA [gal]		ONF [Hz]		GWL [m]
				N	E	N	E	N	E	
App. Pistoiese	23/01/2015	4.3	74	-	-	0.55	2	1.01	1.06	1.99
Emilia	27/01/2012	5	94	-	-	0.18	4.16	0.96	1.02	1.73
Emilia	25/01/2012	5	128	-	-	5.34	4.37	1	1.05	1.75
Costa Toscana	17/04/2006	4.2	33	3.38	4.87	5.17	6.82	0.99	1.01	1.85
Costa Toscana	17/05/2005	4	21	1.26	1.19	1.62	2.27	0.99	1.05	1.79
Garda Sud	24/11/2004	5	214	2.39	3.6	4	8.59	1	1.01	1.98

The analysis confirmed that the mode at 1 Hz is the fundamental bending-type mode of the Tower accounting for the soil-structure interaction (plots E-W and N-S within Figure 5). Such a mode also encompasses a vertical component: indeed, when the Tower bends, the points located away from the axis move vertically as well, which is visible in the vertical component (plot V within Figure 5). On the other hand, the mode at 3 Hz in graph V, basically corresponds

to the vertical mode which is clear in the record of Figure 5. In the horizontal components (graphs E-W, N-S) there is no evidence of a mode at 3 Hz.

Finally, the last graph in Figure 5 [N-S (STR)], obtained by means of the decoupled motion in Equation 3, shows a structural fixed base period on the order of 0.35s. The "fixed base" identified frequencies of the Tower are provided in Table 2. The reader can refer to Kramer et al. (2015) and Karimi et al. (2017) for more information on alternative time-frequency analysis methods.

By analysing the dynamic response recorded during the 27/01/2012 Emilia earthquake, it was established that the natural frequency of the bending mode in the N-S direction is about 0.96 Hz. This value is slightly smaller than the natural frequency of the bending mode in the E-W direction which is close to 1.02 Hz.

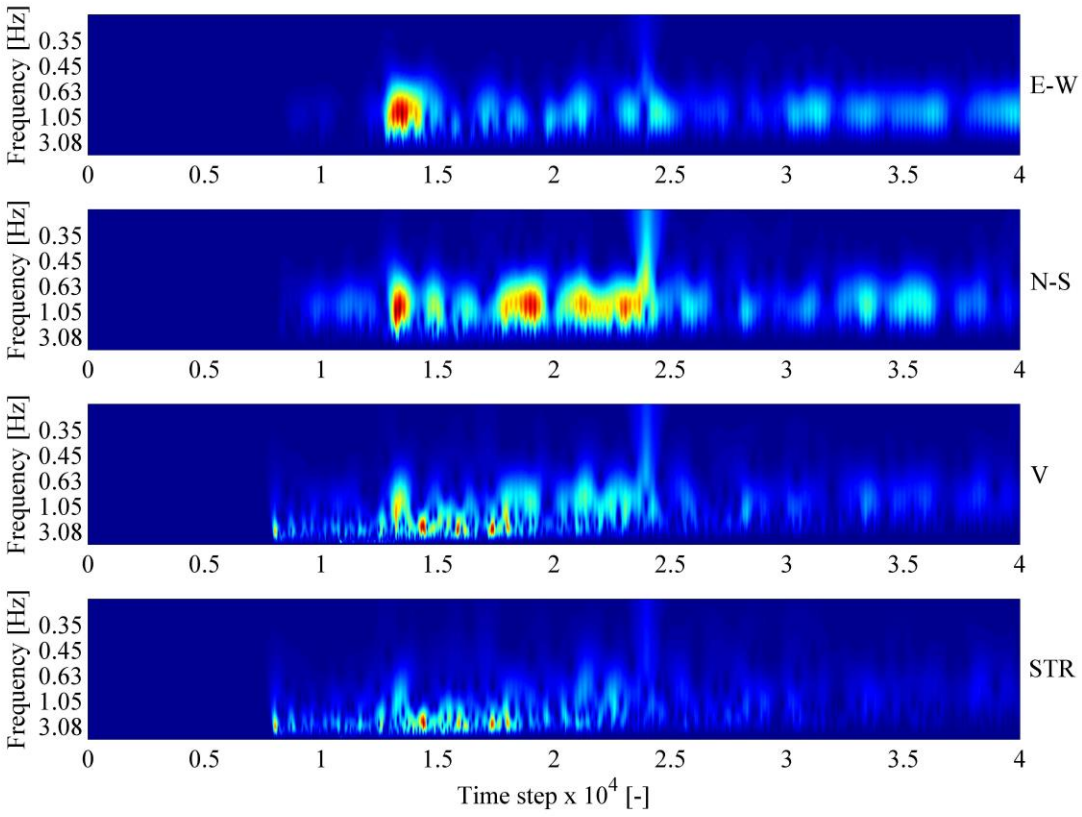

Figure 5. Continuous Wavelet Transform (CWT) of the seismic response acceleration recorded at station S3 (N-S, E-W, V) and horizontal with fixed base: STR, through Eq.3, using stations S1, S3, S4, during the 27/01/2012 Emilia event.

Table 2. Identified frequencies (in Hz) of the Tower from structural response recorded during the 27/01/2012 Emilia event and comparison with previous studies.

Mode	This study	Nakamura et al. (1999)	Macchi & Ghelfi (2005)	Castellaro & Mulargia (2010)	Atzeni et al. (2010)
1st hor. (NS)	0.96	0.98	1.08	1.00	1.01
2nd hor. (EW)	1.02	1.06	-	1.10	1.04
3rd vertical	2.97	3.00	-	-	
4th torsional (?)	6.29	6.30	6.20	6.50	
5th mode		14.00	6.80	6.70	
STR 1st mode (NS)	3.00				

All available experimental studies – with the possible exception of Macchi and Ghelfi (2005) – confirm this finding (see Table 2). Notably, only the present study and the one by Nakamura et al. (1999) have identified an axial mode at around 3 Hz. The identification of the frequency corresponding to the vertical mode is more uncertain: values slightly lower than 3 Hz have been identified by analysing other recordings (not shown), along with a suspected modest variation in time. This evidence is in agreement with the measurements by Nakamura et al (1999). The last identified mode has a natural frequency of 6.29 Hz. Because of the limited number of sensors, the corresponding mode of vibration cannot be reliably identified. However, based on numerical analysis to be discussed later in this paper, this mode is probably associated with torsion. Despite the different loading conditions under which the dynamic response of the Tower was recorded and the different instrumentation employed, the results of Table 2 do not demonstrate significant differences in natural frequencies among the existing studies.

The foundation rocking can be assessed by filtering the vertical acceleration time histories recorded in stations S1 and S4 within the frequency band of interest (Figure 6). It can be observed (Figure 6, top plot) that the bending-induced vertical response in two opposite points at the base of the Tower is essentially out of phase. On the other hand, the vertical responses at the same points (Figure 6, central plot) due to the vertical mode are nearly identical. Therefore, the bending mode encompasses a strong rocking component, while the vertical one does not involve base rotation. The vertical motion at S1 and S4 obtained by removing the average vertical motion w_0 from the original recordings of each sensor is also shown (Figure 6, bottom plot). Once again, it can be concluded that the responses in S1 and S4 are out of phase each other.

SUBSOIL MODEL

Geophysical analyses

According to available maps, the geologic bedrock under the town of Pisa consists of marine clays located as deep as 500 - 1000 m. However, none of the previous geophysical studies reached a depth larger than 60 m. To explore higher depths, an extended 2D geophysical array (SESAME, 2005) was installed on Piazza del Duomo. The tests were performed by positioning the sensors in a triangular configuration, with the largest and the smallest dimensions fixed to reach higher depths and prevent aliasing. This kind of setup is particularly suitable for applications like the one at hand because it is based on ambient vibration measurements, thus induces minor interference and environmental impacts. The same velocimeters are used to infer the H/V ratio of the site (Nakamura 1989) and validate the hypothesis of horizontal soil layering.

The measurements were performed using nine REFTEK130 stations equipped with Lennartz-3D/5s. The 2D array was installed on the West side of the square (Figure 7).

The adopted array has a triple equilateral triangle geometry with the central station located near the Baptistery (Figure 7). The external triangle is used to reach large depths, while the internal triangles are employed to prevent spatial aliasing (Wathelet et al. 2004). In this way, the subsoil can be accurately characterized up to a depth of about one half the maximum dimension of the triangle. Considering the change in properties at a depth of 100 m (Viggiani and Pepe 2005), the array was designed for a maximum dimension of 200 m.

The software package GEOPSY was used for data analysis. The spectral ratios of the horizontal and vertical components (H/V) of the noise field (Nakamura 1989, 2000) were computed for all stations to identify the fundamental frequencies where energy is concentrated (Lermo and Chavez Garcia 1993), Figure 7. All the (H/V) curves were computed using an anti-trigger software to eliminate punctual sources and consider solely ambient noise (SESAME 2003). The (H/V) ratios exhibit two main frequencies: one at 0.3 Hz and a second at 1.3 Hz. Since the natural frequency in shearing oscillations of a homogeneous soil layer is $V_S/(4\Delta h)$ (Δh being the thickness of the layer), the frequencies found by means of the (H/V) ratio can be related to the depth of the interfaces between one layer and the one below. The peak at 1.3 Hz was considered here, and it is related to the interface between the layers at the depth of 40 m. Similar results have been obtained by Nakamura et al. (1999) who identified a frequency at 1.2 Hz, and by Castellaro and Mulargia (2010) who found a peak at 0.3-0.4 Hz and another one at

1.1 Hz. Regarding the lower frequency peak (which can be associated with a deeper interface), it can be argued that the seismic bedrock lies at a depth of about 500 m. Since there is no data at such depths, the peak at 0.3 Hz is not considered in the herein reported results.

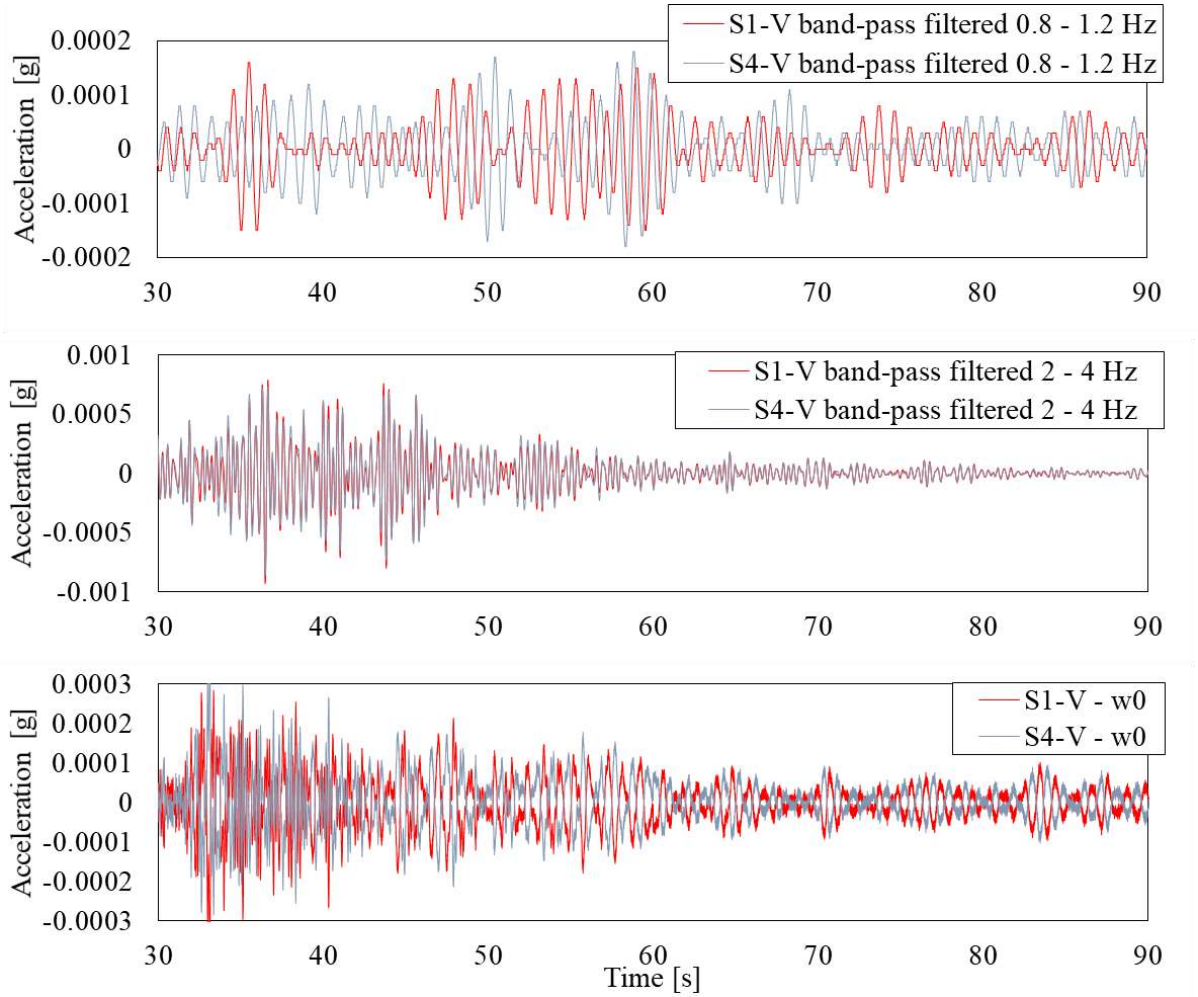

Figure 6. Vertical seismic response recorded at S1 and S4 during the 27/01/2012 Emilia event after the application of a Butterworth band-pass filter. The filtering operation is intended to isolate the dynamics of the first fundamental mode (top) and that of the first vertical mode (center). Vertical motions of S1 and S4 sensors obtained by removing the average vertical motion (bottom).

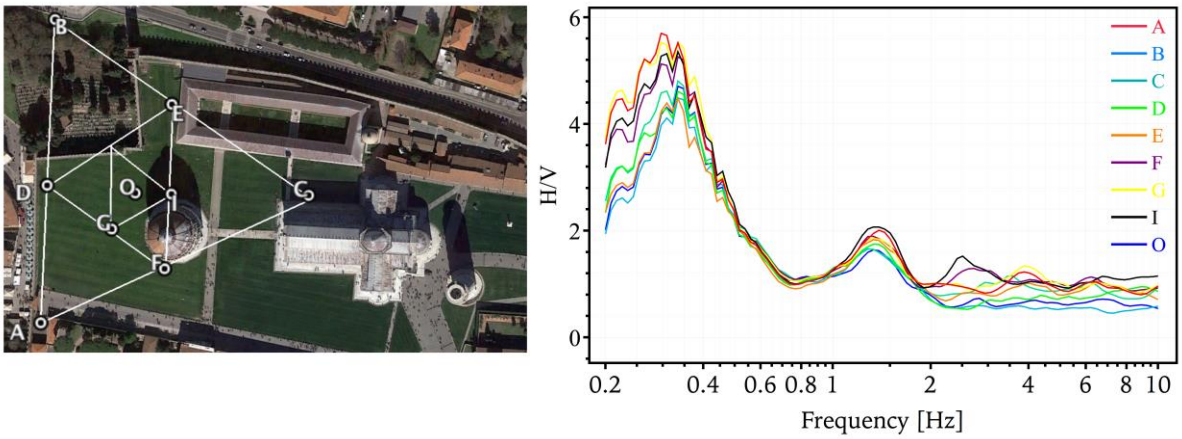

Figure 7. 2D array test performed in Piazza del Duomo: geometry of the array (left), H/V function of the stations (right).

As the (H/V) peaks are the same for all stations in the array, it is confirmed that the near-surface geology for the area can be modelled by horizontal layers. Considering that ambient vibrations are mainly composed by surface waves and that Rayleigh waves are predominant in the vertical motion (Tokimatsu 1995), the Rayleigh wave dispersion curve, which provides the slowness of the Rayleigh waves versus frequency, has been computed using 120 minutes of noise recording in the vertical direction through the high-resolution f-k technique (Capon 1969). The dispersion curve was established by means of an inversion algorithm (Sambridge 1999; Wathelet et al. 2004) to provide the shear wave velocity profile (V_S) of the site (Figure 8a). The inversion process was implemented by constraining the surface shear wave velocities based on those evaluated from available geophysical tests.

The comparison of Vs values obtained from all available geophysical tests is shown in Figure 8a. The inversion for the subsoil profile was improved in this work by combining the vertical shear wave velocity profile obtained from the new geophysical data, local geological conditions and the results of previous geophysical tests. In general, there is a satisfactory agreement among all available tests.

The new data obtained as part of this study were successful in identifying an interface at 100 m transitioning to a layer with V_S = 500 m/s. This is a new result, since previous tests achieved a maximum depth of about 65 m. Three main layers A, B and C can now be identified. These could be further subdivided into several sub-layers according to the available geotechnical information.

Please note that the absence of a base layer with $V_S \geq 800$ m/s, the term “seismic bedrock” is used in the ensuing to indicate the layer with $V_S \approx 500$ m/s (Soil B according to Eurocode

8). This seismic bedrock was adopted in the site response analyses, as described in Yoshida (2015).

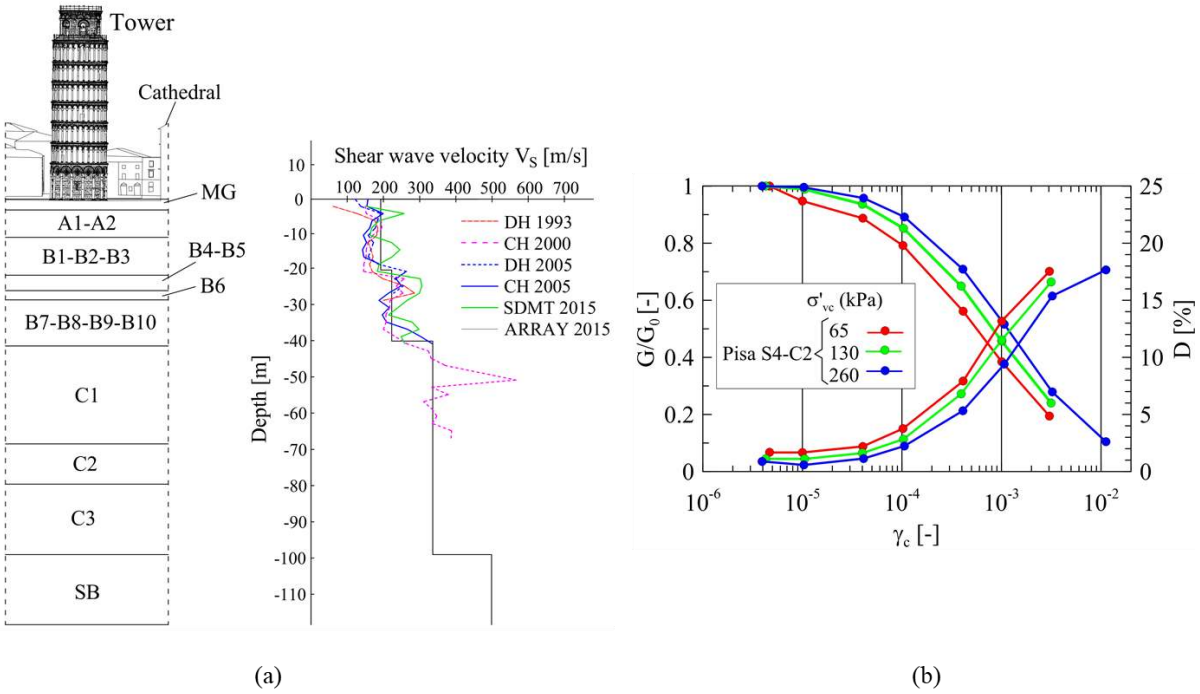

Figure 8. (a) Proposed soil profile model (left); V_S values obtained using different techniques (right), (b) G/G_0-γ_c and D-γ_c through DSDSS test on S4-C2 sample for soil A1 at 6.3 m depth.

Geotechnical tests and numerical subsoil model for site response analysis

The subsoil model adopted for site response analyses is reported in Table 3.

A stratigraphy for the Tower area was proposed by Viggiani and Pepe (2005) based on a number of geotechnical investigations carried out from 1907 to 1993. This model has been validated by geophysical tests performed as part of this investigation. Three distinct horizons are considered, namely A (sandy and clayey silts), B (marine clays) and C (dense sands), which are further subdivided into the zones listed in Table 3. Thickness Δh and unit weight γ for each layer are assumed according to the data reported in Viggiani and Pepe (2005). The adopted shear wave velocity profile V_S is based on the geophysical data as part of the present study.

The profile of compressional wave velocity V_P through the soil skeleton is defined from the V_S profile by assuming for each layer average values of Poisson's ratio measured in the CH test. Regarding nonlinear properties, most soil samples were characterized based on the resonant column (RC) tests (Impavido et al. 1993). The layer A1 (for which no cyclic data is

available) was characterized within the present work through cyclic DSDSS (Double Specimen Direct Simple Shear) tests (D'Elia et al. 2003) performed on a soil sample retrieved from a depth of 6.3 m. The cyclic tests have been conducted at various vertical effective consolidation stresses σ'_{vc} (65, 130 and 260 kPa, corresponding to depths of 3.5, 7 and 14 m, respectively) and the corresponding results are reported in Figure 8b in terms of normalized shear modulus and damping ratio as a function of the shear strain amplitude (i.e., G/G_0-γ_c and D-γ_c curves). Due to a lack of experimental data, literature curves obtained for similar soils were employed for the remaining cases (Darendeli 2001; Rollins et al. 1998 - see Table 3).

Table 3. Subsoil model adopted for site response analyses (ST = Stratum, NL = nonlinear characterization, PI = plasticity index, MG = man-made ground, SB = seismic bedrock, σ'_{vc} = vertical effective stress).

ST	Δh (m)	γ (kN/m^3)	V_S (m/s)	V_P (m/s)	NL
MG	3.0	18.50	180	1650	Average (Rollins et al. 1998)
A1	5.4	18.94	180	1650	DSDSS test, σ'_{vc} = 66 kPa
A2	2.0	18.07	180	1650	PI=30, σ'_{vc} = 55 kPa (Darendeli 2001)
B1	3.5	17.00	180	1650	RC tests
B2	2.0	17.49	180	1650	RC tests
B3	4.9	16.67	180	1650	RC tests
B4	1.2	19.48	230	1730	RC tests
B5	3.0	19.76	230	1730	RC tests
B6	2.4	19.11	230	1730	PI=8, σ'_{vc} = 200 kPa (Darendeli 2001)
B7	4.6	18.62	230	1730	RC tests
B8	1.4	18.41	230	1730	RC tests
B9	4.0	19.01	230	1730	RC tests
B10	2.6	19.38	230	1730	RC tests
C1	27.6	20.52	340	1730	PI=0, σ'_{vc} = 350 kPa (Darendeli 2001)
C2	11.1	20.52	340	1730	PI=15, σ'_{vc} = 500 kPa (Darendeli 2001)
C3	16.3	20.52	340	1730	PI=0, σ'_{vc} = 600 kPa (Darendeli 2001)
SB (C3)	-	21.00	500	2500	linear

SEISMIC INPUT AND SITE RESPONSE ANALYSIS

Definition of seismic input

The area around Pisa is characterized by moderate seismicity. The main seismic sources in the vicinity are located close to Pisa hills (which released the 1846 M 6 Orciano Pisano earthquake) and the Garfagnana area (which triggered the 1920 M 6.5 Garfagnana earthquake). According to the Italian Database of historic earthquakes (Rovida et al., 2016), eight

earthquakes with intensity (I_{MCS}) greater than or equal to 6 struck Pisa since 1117 AD. Seven events took place after the completion of the Tower (1370), therefore the Tower has withstood a considerable number of earthquakes with I_{MCS} ranging from 6 to 7.

The strongest earthquake which took place during the life of the Tower is the August 14 1846 M 6 event, which is known as the Orciano Pisano earthquake. Damage observed in the town of Pisa during this earthquake is reported by Leopoldo Pilla[2] (1846), a famous geologist-mineralogist and Professor at the University of Pisa. Pilla reports that the vault of the church of S. Michele collapsed and there was damage to a vault in the church of S. Francesco. Cracks were also observed on the Clock Tower of *Palazzo Pretorio*, in the columns of the peristyle. In the *Piazza del Duomo,* one cross of the roof and a marble square stone of the outer wall of the *Duomo* fell down. Some light cracks were observed in the *Camposanto* (Cemetery) and the *Battistero* (Baptistry). No damage was observed on the Tower of Pisa (*Campanile*), despite its precarious condition.

To define the surface ground motion through site response analysis, it is first necessary to assess the seismic hazard. Given the results obtained in the previous sections, the seismic input is evaluated assuming a bedrock of type B ($360 < V_{S30} < 800$ m/s). The identification of a deeper ($h >> 100$ m) rigid bedrock, corresponding to type A ground conditions ($V_{S30} > 800$ m/s) is also explored. The seismic hazard assessment was carried out by combining a probabilistic approach (PSHA) and a deterministic one (DSHA). The PSHA has been performed with the software CRISIS (Ordaz et al. 2014) adopting the seismic zonation ZS9 (Meletti et al.2008) and the seismic catalogue CPTI04 (Gruppo di lavoro CPTI 2004) used for the development of the national seismic hazard map (Stucchi et al. 2004). The adopted Ground Motion Predictive Equation (GMPE) is AB10 (Akkar and Bommer 2010). The hazard curves for the site of Pisa confirm the findings of Grandori and Faccioli, that the return periods corresponding to the PGA values associated to macro-seismic intensities of VI and VII degree are, respectively, 130 and 500 years.

[2] Leopoldo Pilla was a liberal and polymath who favoured the Risorgimental ideals of the first part of the 19th century. He was killed in the historic battle of Curtatone (5/29/1848), while commanding the First Company among the Volunteers of the Pisa University Battalion against a vastly superior Austrian Army, during the first war of Italian Independence.

The hazard disaggregation provides the intervals of magnitude and distance that correspond to the highest contributions: for a return period T_R = 130 years, earthquake magnitude M = 5.0-5.2 and epicentral distance R = 0 - 15 km; for T_R = 500 years, M = 5.4 - 5.9 and R = 0 - 25 km. Two earthquakes corresponding to the above listed M - R intervals have been identified in the seismic catalogue: a M_W 5.1 event with R = 19 km was selected for T_R = 130 years (Livorno 1742), and a M_W 5.7 earthquake with R = 21 km (Orciano Pisano 1846) has been considered for T_R = 500 years. Figure 9 shows a comparison between deterministic (DS) and probabilistic response spectra (UHS) of the horizontal component obtained for Soil A and Soil B conditions, respectively. Note that the probabilistic spectra encompass the contribution of several seismic events and incorporate the standard deviation of the adopted GMPE. Following Bommer and Abrahamson (2006), Sabetta et al. (2005) and Sabetta (2014), the deterministic spectra are scaled by a pertinent fraction of the GMPE standard deviation to fit the corresponding probabilistic spectra. Evidently, the response spectra on Soil A and Soil B are quite similar. It is worth noting that the response spectra on Soil B have larger ordinates, mostly at long periods.

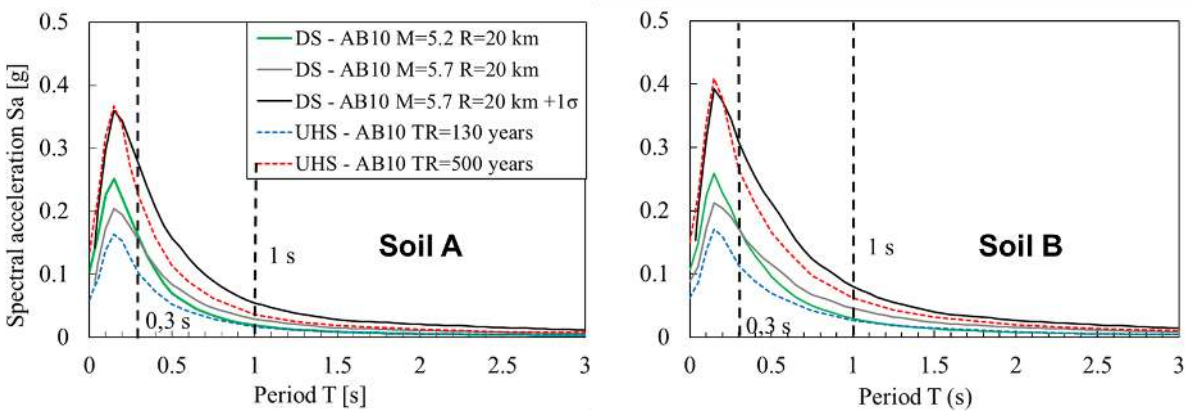

Figure 9. Probabilistic (UHS) and deterministic (DS) response spectra in Pisa: Soil A (left) and B (right). Dashed black lines: periods of the fundamental bending modes of the Pisa Tower.

Based on these results, it is possible to argue that the two deterministic spectra lie within the ordinates of the probabilistic ones. According to the disaggregation, it seems reasonable to adopt the median value obtained from GMPE of Livorno 1814 earthquake for T_R = 130 years, and the median value plus one standard deviation for the Orciano Pisano 1846 earthquake, to obtain a good agreement between the DS and the UHS at T_R = 500 years.

Seven accelerograms recorded on type B soil have been selected from the European Strong Motion Database (Luzi et al. 2016) in the M-R intervals reported above for T_R = 130 years and 500 years. The accelerograms have been scaled in such a way that the average spectrum of

each set matches the target spectrum. This was accomplished by using the software In-Spector (Acunzo et al. 2014). The scaling was made in the range of fundamental periods 0.3-1.1 s to consider the periods of the first two bending modes of the structure (about 1 s) and that of the third (vertical) mode (about 0.3 s), thus obtaining the proper scale factor (SF) for each record (Figure 10 a-b). For T_R = 130 years the average spectrum of the scaled records approximates well the target spectrum for all spectral periods. On the other hand, for T_R = 500 years there are larger differences in spectral values up to T = 0.3 s, while between 0.5 s and 1.1 s the differences are smaller. This is because the strong motion records were scaled to obtain a good match at T = 1 s, since they attain small values at long periods. Moreover, for both return periods the average values ± one standard deviation were also evaluated, to highlight the dispersion of the input strong motion records. It can be observed that for T_R = 500 years there is significant dispersion of the ordinates in the range T = 0 - 0.5 s, while the dispersion is smaller at longer periods.

Tables 4 and 5 list the parameters of the scaled accelerograms for T_R = 130 years and 500 years, respectively. In addition to the relevant parameters of the seismic events, the scale factor (SF) used for each record and the average root-mean-square deviation of the response spectrum of the scaled records from the target design spectrum D_{rms} in the period range 0.3 - 1.1s (Bommer and Acevedo 2004) are provided.

To obtain the vertical time histories on soil B, each original vertical record taken from the European Strong Motion Database has been scaled with the corresponding SF obtained for the horizontal components (see Figure 10 c-d). In this case, for T_R = 130 years the data dispersion is quite large, while for T_R = 500 years the dispersion is smaller in comparison to the horizontal motion. Note that the implemented methodology has some advantages over the approach adopted by Grandori and Faccioli (1993). Firstly, the Italian Database at the time contained a limited number of records and stations. Secondly, the accelerograms were selected based on magnitudes between 5.4 and 6.8, which is less consistent with the earthquake scenario expected for T_R = 130 years. Thirdly, Grandori and Faccioli (1993) scaled the selected accelerograms to achieve a PGA of 0.07g instead of performing the calibration based on the natural periods of the structure. Conversely, the present work is based on a larger, up-to-date strong-motion database. The records correspond to seismic events having magnitude between 5 and 5.5, in agreement with the earthquake scenario expected for T_R = 130 years. The records were scaled

to obtain a best fit within the range of natural periods of the Tower. The final goal of the implemented approach was to obtain horizontal and vertical seismic action on the free field.

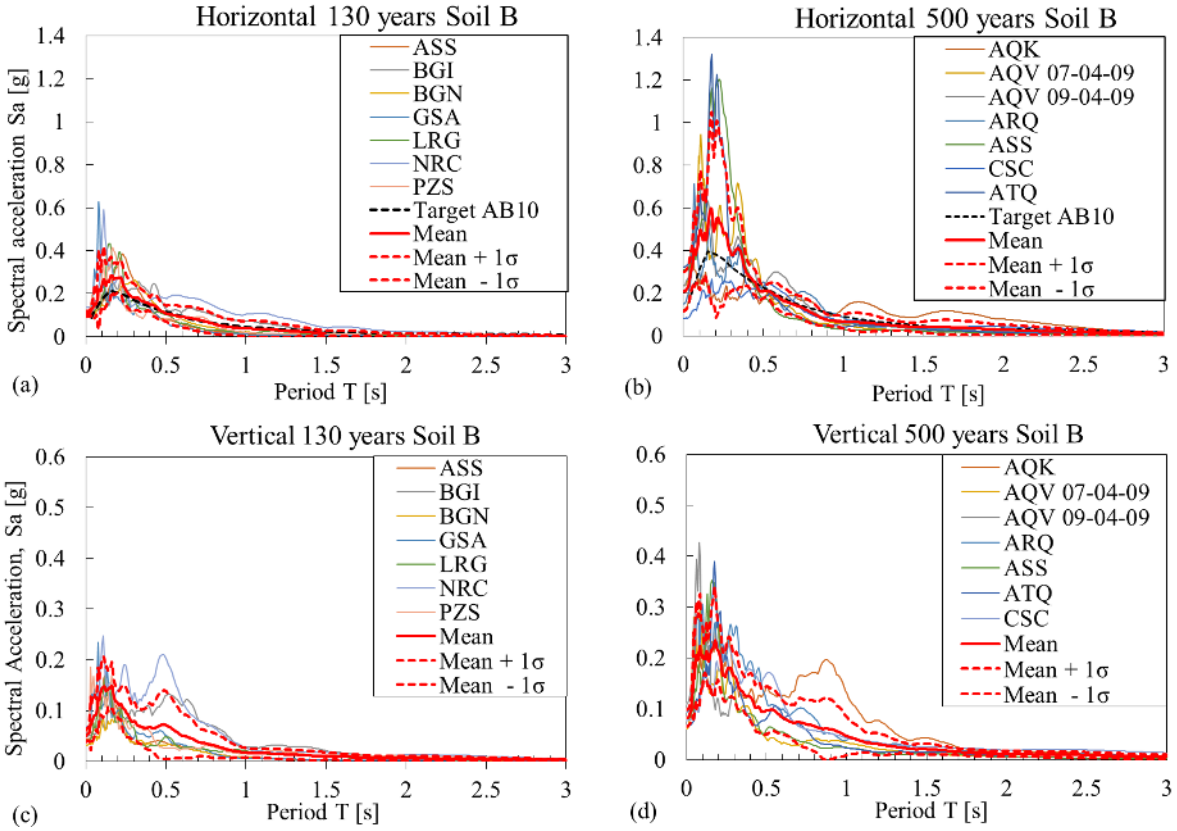

Figure 10. Response spectra of scaled accelerograms**:** horizontal (a-b) and vertical (c-d) components. σ = Standard Deviation.

Table 4. Selected accelerograms for T_R=130 years; R = Distance from source; SF = Scale Factor; D_{rms} = Root Mean Square deviation from target spectrum.

Event	Date (dd/mm/yy)	Station	M	R [km]	Soil	$V_{S,30}$ [m/s]	SF	D_{rms}
Umbria-Marche	03/10/1997	ASS	5.2	20.3	B	-	1.08	0.051
Irpinia	24/11/1980	BGI	5.0	17.2	B	498	3.00	0.049
Emilia	27/01/2012	BGN	5.0	22.3	B	640	2.09	0.029
L'Aquila	09/04/2009	GSA	5.2	16.7	B	492	2.13	0.038
Pollino	25/01/2012	LRG	5.2	19.5	B	603	2.66	0.037
Umbria-Marche	12/10/1997	NRC	5.2	18.8	B	498	2.00	0.052
Garfagnana	21/06/2013	PZS	5.1	13.8	B	453	1.11	0.039

Site response analysis at seismic bedrock

Site response analysis provides information about the amplification of seismic motion. The evaluation of free field motion requires establishing at least three translational components. To

this end, two types of analysis were carried out: i) a conventional approach considering solely vertical S wave propagation, which disregards vertical ground motion, ii) a 2D finite element response analysis for combined horizontal and vertical motion at the base.

Table 5. Selected accelerograms for T_R=500 years; R = Distance from source; SF = Scale Factor; D_{rms} = Root Mean Square deviation from target spectrum.

Event	Date (dd/mm/yy)	Station	M	R [km]	Soil	$V_{S,30}$ [m/s]	SF	D_{rms}
L'Aquila	09/04/2009	AQK	5.4	16.5	B	705	2.50	0.045
L'Aquila	09/04/2009	AQV	5.4	12.4	B	474	1.50	0.031
L'Aquila	07/04/2009	AQV	5.5	14.3	B	474	1.60	0.054
Norcia	19/09/1979	ARQ	5.8	21.0	B	-	2.00	0.029
Umbria-Marche	26/09/1997	ASS	5.7	24.2	B	-	2.00	0.074
Lazio-Abruzzo	11/05/1984	ATQ	5.5	17.4	B	-	2.00	0.077
Umbria-Marche	14/10/1997	CSC	5.6	24.3	B	698	1.31	0.093

Initially, site response analyses have been carried out using the 1D frequency-domain equivalent linear STRATA code (Kottke et al. 2013), by applying the horizontal component of ground motion. The analyses were then repeated with the 2D equivalent-linear finite element code QUAD4M (Hudson et al. 1998) using both horizontal and vertical components of the selected accelerograms. These analyses have also allowed computing the vertical component of the seismic motion at the ground surface. The same subsoil model employed for STRATA (with horizontal layering) is assumed in QUAD4M.

Figure 11 shows results of the site response analyses, in terms of response spectra, for the horizontal and vertical components. Figure 11a depicts results for the horizontal component and T_R = 130 years. First, by comparing the average amplified spectrum with the input spectrum for Soil B, it is possible to notice a large amplification extending from 0.3 s to 2 s. Average response spectra ± one standard deviation are also displayed (red dashed lines) and demonstrate a significant dispersion in the results. The comparison between the average plus one standard deviation and the response spectrum obtained by Grandori and Faccioli (who used the same representation) shows that the former spectrum has larger ordinates until 1.4 s. The fundamental natural period of the Tower corresponds to a horizontal acceleration of 0.15g and 0.11g in the two spectra, respectively, corresponding to a discrepancy larger than 20%.

Figure 11b shows results for T_R = 500 years. In this case the amplification starts from T = 0.2 s and extends to 2 s. It is worth noting that, for this return period, there is a larger dispersion

in spectral values at low natural periods. For T = 1 s, the spectral acceleration is 0.15g and 0.20g, for the amplified average spectrum and the average spectrum plus one standard deviation, respectively.

Figure 11c shows results for the vertical surface motion component corresponding to T_R = 130 years. Evidently, there is a strong amplification below T = 1s. The comparison between the spectrum obtained by Grandori and Faccioli and the average amplified spectrum + one standard deviation shows that the ordinates of the former are smaller than those of the latter for all the considered periods. The natural period of the Tower in the vertical direction corresponds to an acceleration of 0.12g and 0.1g in the two spectra, respectively. Figure 11d depicts spectral accelerations for T_R = 500 years, corresponding to 0.24g at 0.3 s (average value) and 0.3g (average value plus one standard deviation).

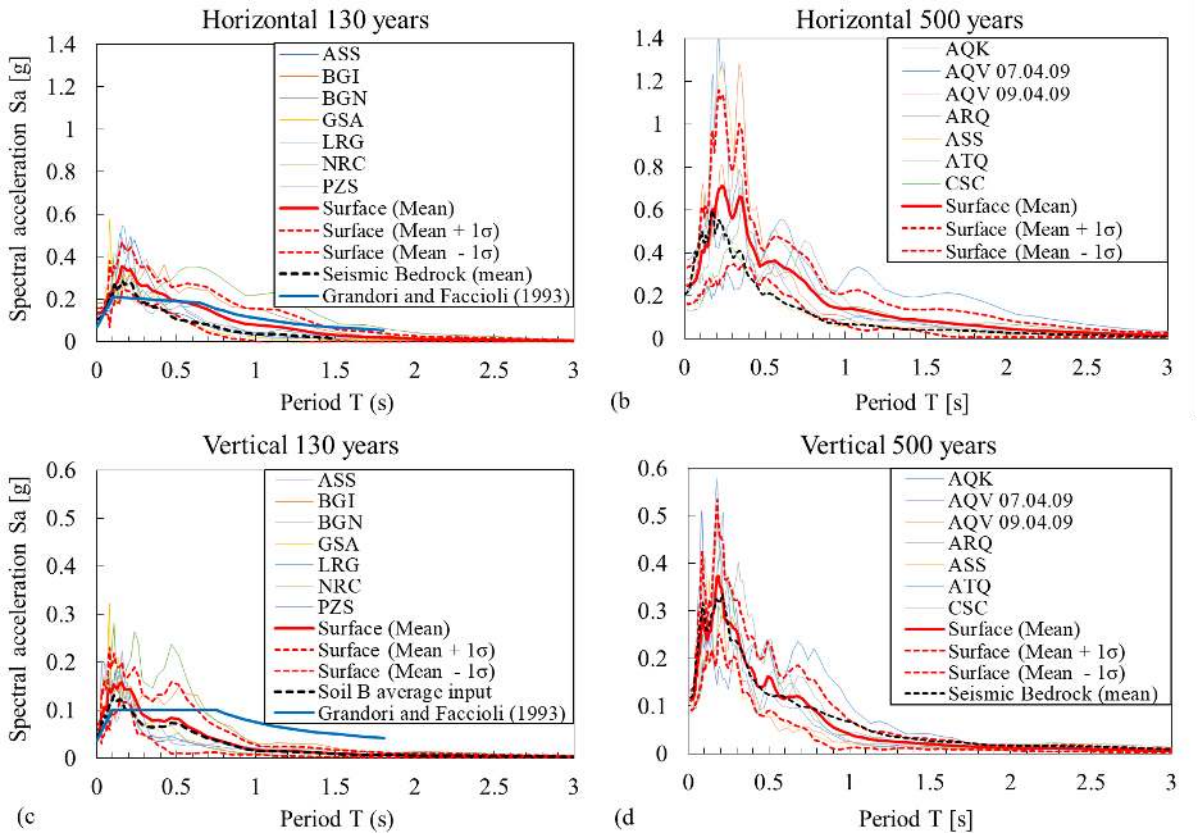

Figure 11. Response spectra free field/input**:** horizontal (a-b) and vertical (c-d).

In Figure 12, the average amplification functions for horizontal and vertical components are reported. Major amplifications as high as 2 are observed around 1 Hz for the horizontal component, while motions at frequencies beyond 7 Hz are damped. As expected, a stronger nonlinear behavior appears in the horizontal component for T_R = 500 years, thus resulting in

stronger damping at high frequencies. The vertical component is moderately amplified with a maximum value of 1.5 at around 5 Hz.

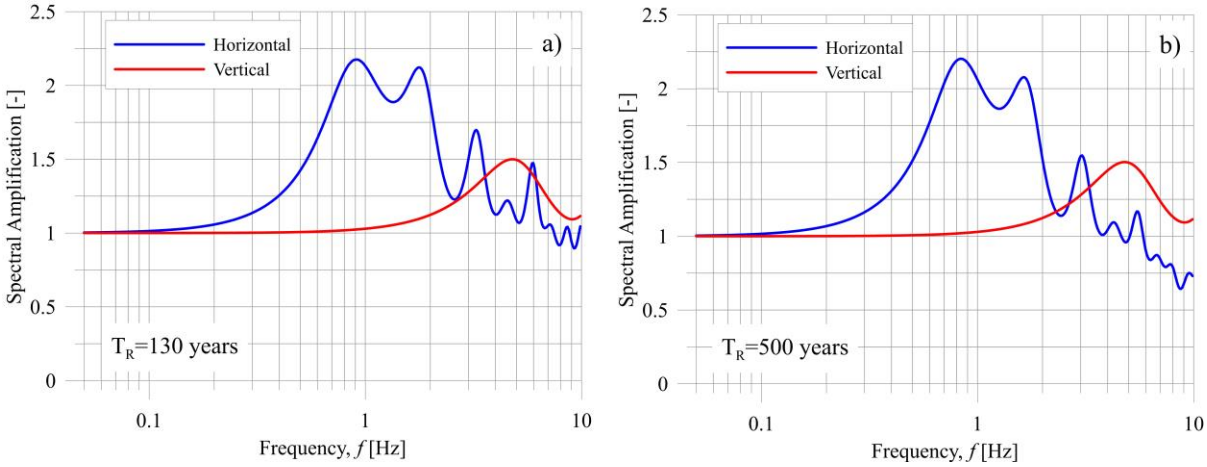

Figure 12. Average amplification functions at ground surface: T_R=130 (a) and 500 (b) years.

SIMPLIFIED STRUCTURAL MODEL

Finite element model of the superstructure

Considering the Tower to be sufficiently slender to exhibit flexural behavior, a simplified 3D elastic finite-element model was developed using the program SAP2000. The model consists of beam elements accounting for stiffness variation with height, for a total of 54 dynamic degrees of freedom with masses concentrated in 9 nodes (Figure 13a). In the model, the inclination of the Tower varies with height following that of the prototype.

Geometric data and inertial parameters have been defined according to Macchi and Ghelfi (2005). The coordinates of the centroid for each level reflect the actual inclination of the Tower. The parameters assigned to the numerical model are reported in Figure 13b.

Specifically, the inclination along the North-South direction (y_i coordinate) is considered, whereas the (minor) inclination in the East-West direction (x_i) is neglected. Areas and second moments of inertia have been homogenized by assuming the hollow sections to be made of marble with elastic modulus and Poisson's ratio of 80 GPa and 0.3, respectively.

The results of these tests are summarized by Macchi and Ghelfi (2005), and were adopted in our study. The fixed-base structural properties reproduce satisfactorily the experimentally measured natural period of 0.35s in the lateral mode (Figure5, Table 2), while the 0.065s period in the axial mode, seems too short to be catch with the present arrangements.

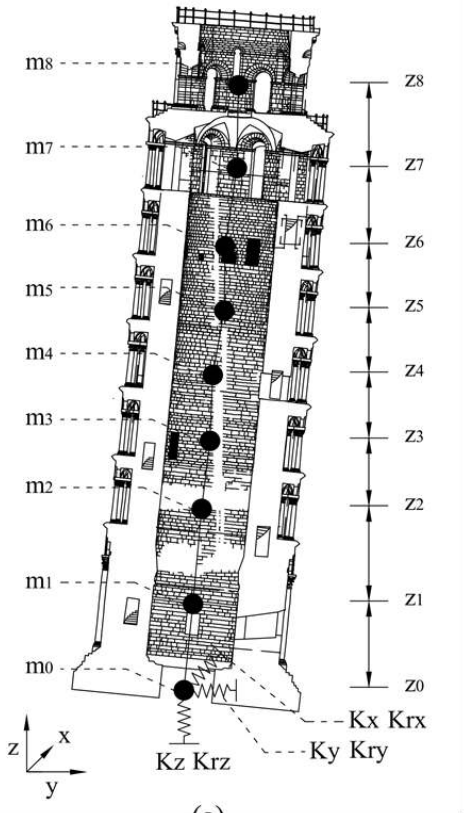

(a)

Level	x_i [m]	y_i [m]	z_i [m]	m_i [Mg]	A_i [m^2]	J_i [m^4]
0	0.02	0.18	1.8	2350	---	---
1	0.01	0.94	9.4	3750	35.7	763
2	0.21	1.70	17.9	1380	28.3	443
3	0.21	2.45	23.8	1380	28.3	443
4	0.13	2.68	29.7	1230	21.4	388
5	0.00	3.72	35.4	1210	21.4	388
6	0.06	3.79	41.1	1160	21.4	388
7	0.18	4.82	47.9	1240	20.4	352
8	0.12	5.02	55.3	698	16.5	230

(b)

Figure 13. (a) Finite element model, (b) x_i, y_i, z_i of the centroids; m_i: mass; A_i: element area; J_i: element bending moment of inertia.

At first approximation, the soil underlying the Tower is modelled as a homogeneous elastic half-space, with mass density ρ and shear wave velocity V_S equal to 1.87 Mg/m^3 and 200 m/s, respectively (average free-field values within a depth of 35 m or two foundation diameters). For small deformations, the shear modulus of soil can be evaluated as $G_0 = \rho V_S^2$, which provides a nominal value of 77 MPa.

Given the lack of sensitivity of the foundation impedances to Poisson's ratio of soil, ν was taken equal to 0.5 corresponding to fully saturated conditions. It should be noted that taking ν= 0.45 yields minor variations in the values of the springs, on the order of 3-10%.

Foundation impedances and calibration

Three translational and three rotational springs were assigned at the base of the model (Fiorentino et al. 2017), corresponding to a shallow ring foundation without embedment.

Given the relatively small size of the foundation and the lack of embedment, kinematic interaction effects associated with wave scattering were neglected (Mylonakis et al. 2006,

NIST 2012). Also, the off-diagonal elements of the foundation impedance matrix are negligible, therefore inertial interaction was modelled based solely on the diagonal terms in translation and rotation. As the foundation has a ring shape, the resulting impedances were obtained by subtracting the area and moment of inertia corresponding to the inner radius from those corresponding to the outer one, in the related modes. Two different cases are examined below:

- a ring-shaped foundation considering the Tower only (i.e. excluding the Catino),
- a ring-shaped foundation considering both the Tower and the Catino.

In the latter model, the Catino is assumed to be rigidly linked to the foundation in horizontal translation and torsion. In reality the link between the Catino and the Tower is uncertain because of the (unknown) rigidity of the interface of the two components and the pre-tensioned radial system. The Catino has a high stiffness on its own plane (i.e. in horizontal translation and torsion) and a low stiffness out of plane (in vertical translation and rocking). For the elastic shear modulus of soil, two values are considered: i) the nominal value, $G_0 = 77$ MPa, obtained from V_S, as discussed earlier; ii) a corresponding value of G obtained from a sensitivity analysis to minimize the difference between the experimental and the numerically evaluated natural frequencies. The best estimate coming out of this exercise is $G_0 = 95$ MPa, which allows a good matching between the numerical frequencies and those identified experimentally for the first three vibration modes. Using the latter value of shear modulus, the corresponding shear wave velocity was estimated at around 225 m/s, which is consistent with the subsoil model in Figure 8 and accounts for the overburden effect due to the weight of the structure (NIST 2012). Table 6 shows the comparison between the experimental and the numerically evaluated frequencies obtained for the two configurations of the foundation and for the two values of G_0. Table 7 reports the corresponding dynamic impedances.

Table 6. Measured and computed natural frequencies of the Tower with/without Catino. Numerical results for $G_0 = 77$ and 95 MPa.

Mode Direction	Measured (Hz)	Computed natural frequency [Hz]			
		without Catino		with Catino	
		G_0=77 MPa	G_0=95 MPa	G_0=77 MPa	G_0=95 MPa
1st horizontal (NS)	0.96	0.87	0.96	0.88	0.97
2nd horizontal (EW)	1.02	0.87	0.96	0.88	0.97
3rd vertical	2.97	2.82	3.12	2.83	3.13
4th torsional	6.29	4.31	4.73	5.92	6.43

It can be inferred from Table 6 that minor discrepancies still exist in the numerical values of the modal frequencies. To reduce such errors, the calibration of the dynamic impedances of the foundation was also performed by means of a numerical optimization method (Liu et al. 2016; Marano et al. 2011; Monti et al. 2009). Specifically, the method modifies the elements of the foundation stiffness matrix for a best matching between the experimental and numerical frequencies of the 1st and the 2nd bending modes, the vertical mode and the torsional one. In doing so, the lower and upper bound of the dynamic impedances were assumed equal to ±20%, respectively, of the values obtained using the approach by Mylonakis et al. (2006) using G_0 = 95MPa and a foundation with Catino (last column in Table 6). The optimal numerical values of the dynamic impedances are listed in Table 7 and yield numerical frequencies which are essentially identical to the experimental ones. Interestingly, it seems that the presence of the Catino affects only the torsional mode. Useful observations can be made on the impedances reported in Table 7. Regarding the values employed by Grandori and Faccioli (1993), it is worth noting that all terms are smaller than those established in this work, as they were based on a value of G_0 = 58 MPa leading to a fundamental natural frequency of only 0.74 Hz. Conversely, the calibration of the impedances in ISMES resulted in higher values for the translational impedances (K_x, K_y, K_z), while the rotational impedances were like those obtained in this study. It is worth recalling that the ISMES model employed lower values for the material constants of the Tower marble. The importance of soil-structure interaction on the vibrational characteristics of the Tower can be evaluated based on the so-called wave parameter introduced by Veletsos and co-workers (Veletsos & Meek 1974; NIST 2012; Maravas et al 2014).

$$\frac{1}{\sigma} = \frac{H^* f}{V_s} \tag{4}$$

H* being the height of an equivalent SDOF structure (about 23 m based on the elevation of the centre of mass of the Tower), f its fixed base natural frequency (about 3 Hz) and Vs the soil shear wave propagation velocity in the soil (about 225 m/s). Considering these values, the wave parameter is estimated at around 0.3 a remarkably high value which exceeds all available data for building structures (Stewart et al 1999b). The associated flexible base (SSI) natural frequency can be estimated, in an approximate manner, from the familiar expression (Veletsos & Meek 1974; NIST 2012; Maravas et al 2014)

$$\tilde{f} = f\left[1 + \frac{k}{K_x}\left(1 + \frac{K_x H^{*2}}{K_{rx}}\right)\right]^{-1/2} \tag{5}$$

Table 7. Dynamic impedances with and without Catino. Numerical results for G_0 = 77 and 95 MPa, Optimized model (Opt.) of this work vs results of Grandori & Faccioli (GF 1993) and ISMES.

	This work						
	without Catino		with Catino		Opt.	GF1993	ISMES
G_0 [MPa]	77	95	77	95	-	-	-
Transl. EW, K_x [kN/m ×10^6]	3.1	3.8	4.2	5.2	5.9	2.4	1.3
Transl. NS, K_y [kN/m ×10^6]	3.1	3.8	4.2	5.2	4.6	2.4	1.6
Vertical, K_z [kN/m ×10^6]	4.7	5.7	4.7	5.7	5.2	3.2	8.2
Rot. EW, K_{rx} [kNm/rad ×10^8]	3.8	4.7	3.8	4.7	4.6	2.9	6.2
Rot. NS, K_{ry} [kNm/rad ×10^8]	3.8	4.7	3.8	4.7	5.3	2.9	6.2
Torsion, K_{rz} [kNm/rad ×10^8]	3.8	4.7	8.0	9.8	9.4	2.9	5

where k is the stiffness of the superstructure (which can be evaluated as $k = 4\,\pi^2\, m\, f^2 = (4\,\pi^2$ 145,000/9.81 x $3^2 \approx 5.2$ x 10^6 kN/m) and K_x, K_{rx} are the foundation stiffnesses in horizontal translation and rocking (Table 7 – 4th column). Substituting these values into the above equation, one obtains $\tilde{f} \approx 1.1\ Hz$ which is reasonably close to the measured value of 1 Hz (the difference being probably due to the SDOF approximation of the infinite-degree-of-freedom system). The period shift due to SSI, ($\tilde{T}/T \approx 1$ s / 0.3 s ≈ 3), is the largest known for a building structure (Stewart et al 1999b), in agreement with the large value of the wave parameter (1/σ). Note that equation 5 is not sensitive to the values of the stiffness parameters under the square root.

An equivalent analysis can be carried out considering that the natural frequencies in rocking oscillations of a perfectly rigid superstructure under zero foundation translation is f_{ry} = 1/2π (5 x 10^8 kNm / 1.1 x 10^7 Mg $m^2)^{0.5} \approx$ 1.1Hz, the corresponding frequency in swaying of a rigid superstructure under zero foundation rotation is f_x = 1/2π (5 x 10^6 kN/m / 14500 Mg)$^{0.5} \approx$ 3Hz, and the natural frequency of the fixed-base structure is f =1/2π (5.2 x 10^6 kN/m / 14500 Mg)$^{0.5}$ ≈ 3Hz. Combining the above results using Dunkerley's rule

$$\tilde{f} = \left(f^{-2} + f_x^{-2} + f_{ry}^{-2}\right)^{1/2} \tag{6}$$

yields $\tilde{f} \approx 1\ Hz$, which in meaningful agreement with the first estimate.

The role of SSI in the seismic response of the Tower can be assessed with the help of the response spectrum of Figure 14, obtained by means of equivalent linear site response analysis (red curve) as part of this study. Under fixed-base conditions the spectral response is on the order of 0.6g, whereas under flexible-base conditions it drops below 0.15g – a 400% reduction.

Note that this reduction is probably a lower bound, as it does not account for period elongation due to non-linear soil response, the associated increase in damping etc.

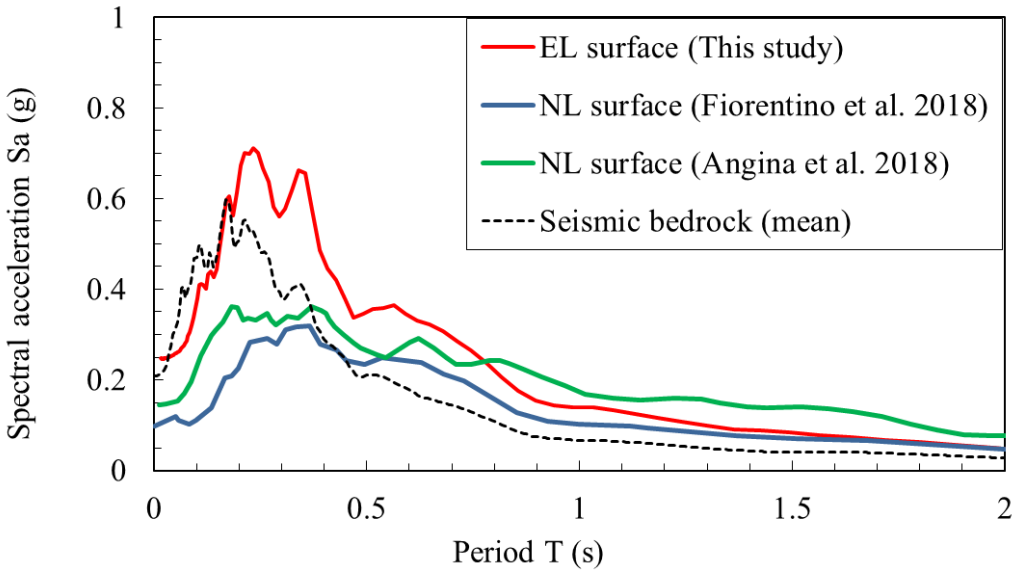

Figure 14. Response spectra at ground surface in Pisa obtained by different authors, highlighting the reduction in seismic response due to Soil-Structure Interaction

It should be noticed that the spectral acceleration with SSI is lower than the PGA of 0.25g (red curve). This suggests that in the realm of the spectrum at hand, a simple oscillator with the particular natural frequency de-amplifies the free field soil motion. Corresponding estimates using nonlinear site response analysis (blue curve) obtained by Fiorentino et al. (2018) indicate a reduction in spectral accelerations due to SSI of about 300% (0.1g over 0.3g), which is in meaningful qualitative agreement with the first estimate. Analogous predictions are obtained with the spectrum by Angina et al. (2018) which indicate a reduction in response due to SSI of about 230% (0.15g over 0.35g). Evidently, the beneficial effect of SSI on the seismic response of the Tower of Pisa can hardly be overstated.

MODAL ANALYSIS AND SEISMIC RESPONSE

Although the instrumentation of the Tower does not allow a full assessment of the modal shapes, some useful conclusions can be drawn on the shapes obtained numerically in this study. Figure 15 (left plot) shows the modal shapes in N-S direction. The normalized modal displacements are added to the undeformed shape and compared with the 1st experimental mode obtained by ISMES, normalized to the same modal displacement at the elevation of the

centroid of the Tower (z = 22.6m). It is possible to observe that the modal shapes obtained in this work are very similar to the experimental ones and are in good agreement with the ISMES modal shape (except possibly near the top of the structure). Figure 15 (right plot) shows modal shapes in E-W direction. It can be observed that all the shapes are consistent, while there are slight differences at the base of the Tower.

A similar good agreement between calibrated and optimized modes can be observed in Figure 16 (left plot) for the vertical mode shapes and in Figure 16 (right plot) for torsional ones. A possible exception is the torsional mode shapes obtained for G_0 = 77GPa, for which higher values of twist are obtained at the base relative to the other cases.

An elastic response spectrum analysis was carried out on the optimized model. To this end, four seismic inputs were considered: i) average response spectrum for T_R = 130 years, ii) average plus one standard deviation for T_R = 130 years, iii) average response spectrum for T_R = 500 years, iv) average plus one standard deviation for T_R = 500 years. For each case, the bending moments and the axial loads at the base due to horizontal and vertical input motion were evaluated. The bending moments are displayed in Figure 17a and compared with: (a) the bending moments obtained by Grandori and Faccioli (1993) and (b) those produced by dead loads (283 MNm). Evidently, the bending moments due to the horizontal component of the earthquake are of comparable magnitude to the static moments due to dead loads.

The following observations can be made in light of these results: (i) except for the case of mean response and T_R = 130 years, bending moments due to the horizontal component of the earthquake motion are larger than those due to gravitational loading. For example, in the worst case scenario (T_R = 500 years, average value + one standard deviation), the moment at the base of the Tower caused by the horizontal component of the earthquake motion is more than double the one due to the dead loads, reaching a value of 684 MNm, (ii) the large dispersion in seismic response causes the mean value + one standard deviation moment for T_R = 130 years to shift above that for T_R = 500 years, (iii) the vertical motion seems to make a moderate contribution to the overturning moment, since the response is primarily along the inclined axis of the tower (i.e., not vertical). Therefore, in this mode there is both a vertical and a horizontal displacement, which produce moments that balance each other.

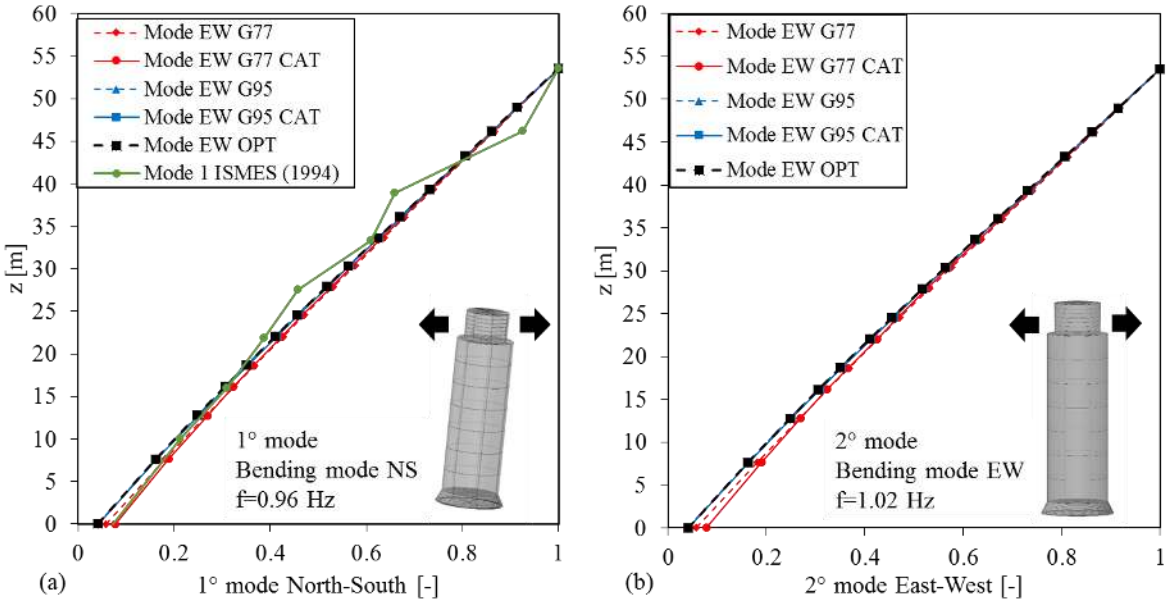

Figure 15. (a) Vibration modes in NS and (b) EW direction. G77, G95: without Catino; G77 CAT, G95 CAT: model with Catino; OPT: optimized model (this work).

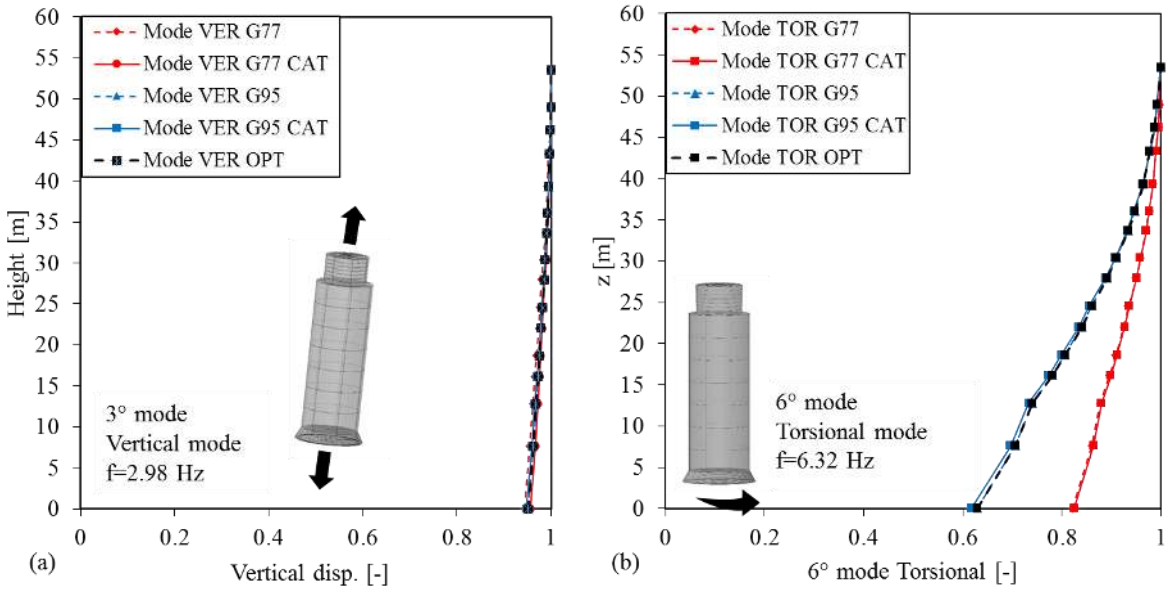

Figure 16. (a) Vibration modes in vertical direction and (b) torsion mode. G77, G95: without Catino; G77 CAT, G95 CAT: model with Catino; OPT: optimized model (this work).

Interestingly, had the horizontal impedances of the foundation been smaller, the bending contribution would be larger, expressed by the ratio of vertical response acceleration to gravity acceleration. For example, for T_R = 500 years a moment corresponding to 30% of the gravity acceleration is obtained. The axial force results displayed in Figure 17b show that the contributions of vertical and horizontal input motion in the worst case scenario (average plus

one standard deviation for T_R = 500 years) are 10% and 30% of the one due to gravity loads, respectively.

The mode shapes obtained using the specific impedances confirm the results of the dynamic identification and are physically consistent. In fact, with the optimized model it is possible to establish a first bending mode in the NS direction (f = 0.96 Hz), a second bending mode in the EW direction (f = 1.02 Hz), a vertical mode (f = 2.98 Hz) and a torsional one (f = 6.32 Hz).

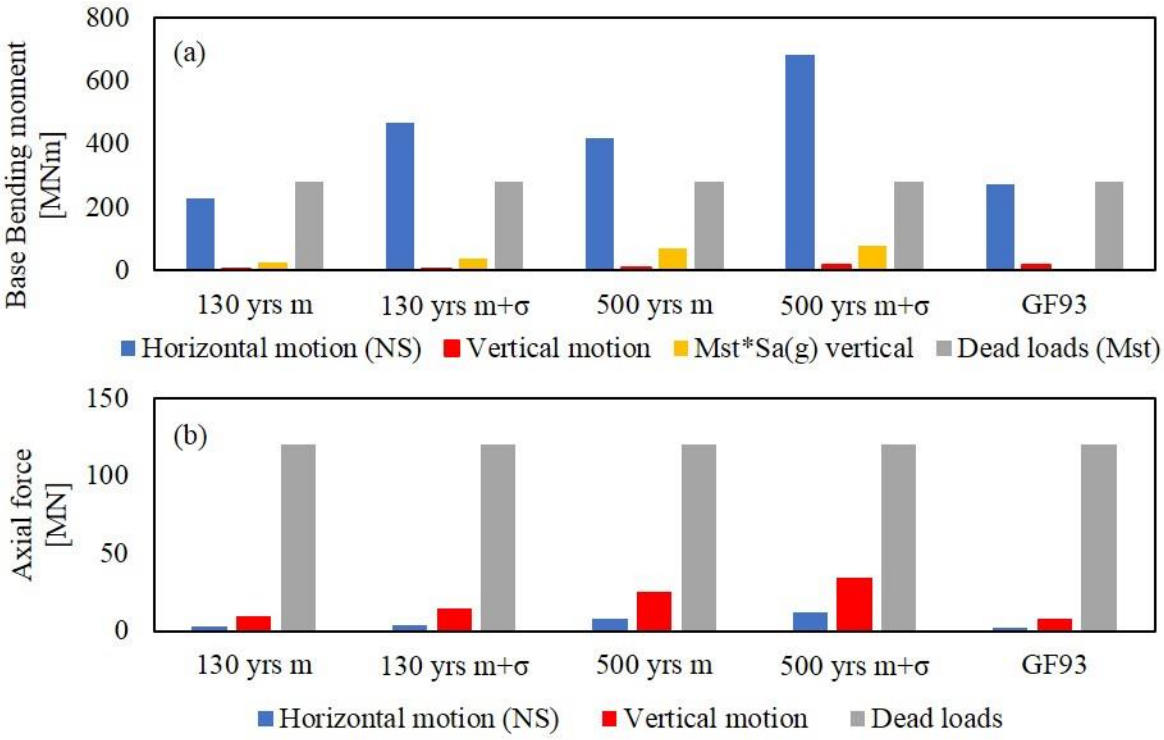

Figure 17. Bending moment (a), Axial force (b) at Tower base due to: horizontal motion (blue), vertical motion (red), vertical motion in case of maximum vertical effect (yellow), and gravity (grey).

CONCLUSIONS

The object of the research was to shed light into the earthquake performance of the Tower of Pisa, which has survived a number of strong events since the middle ages, despite its leaning and vulnerability. To this end, novel experimental and numerical studies on the dynamics of the structure were reported, with emphasis on vulnerability assessment under earthquake action. New contributions include: (a) analysis of seismic structural response data, (b) definition of seismic input on rock and ground surface, (c) geophysical and geotechnical characterization of soil, (d) site response analysis, and (e) calibration of a simplified stick-type finite-element model of the Tower encompassing soil-structure interaction.

Results confirm some of the conclusions reported in previous investigations, such as the natural periods in bending oscillations and the significant seismic demand at the base of the tower. New important findings include assessment of the significance of vertical ground motion, an enhanced subsoil model with "partial" bedrock, and structural response encompassing soil-structure interaction. Furthermore, it seems that a reduction in seismic risk would be possible by both uncertainty reduction and simple intervention strategies (not discussed here). The following specific conclusions were drawn:

(1) The analysis of seismic records identified three vibration modes: two bending modes with frequencies of approximately 1 Hz in N-S and E-W directions, and a vertical mode with frequency of about 3 Hz. The last identified mode has a frequency of 6.29 Hz, which probably corresponds to torsion.

(2) The geophysical tests conducted near the Tower indicate a Soil B layer (Vs = 500 m/s) at a depth of 100 m, while the single station (H/V ratio) indicates two fundamental amplification peaks, one with frequency of 1.3 Hz, corresponding to an interface at approximately 40 m depth, and a second peak with frequency of 0.3 Hz. The latter frequency can be associated with a deep interface transitioning to a very stiff layer, composed possibly of marine clays, at a depth of more than 500 m.

(3) The seismic input was defined in terms of response spectra using a hybrid approach combining Probabilistic Seismic Hazard Assessment (PSHA) and Deterministic Seismic Hazard Assessment (DSHA). The associated response spectra were obtained for both Soil A and Soil B (seismic bedrock at 100 m depth) conditions. Site response analyses were conducted using a subsoil model proposed by the authors, based on the results of the geophysical tests and the geotechnical characterization of the layers using G/G_0-γ_c and D-γ_c curves, specifically developed for the project at hand.

(4) The definition of Soil B type bedrock (instead of a more realistic Soil A type bedrock) induces significant dispersion on the associated GMPE relations. Identifying a Soil A bedrock at a deeper elevation by geophysical means may lead to a reduction in epistemic uncertainty and, therefore, a better estimation of seismic risk of the Tower. Accomplishing this goal lies beyond the scope of the herein reported research.

(5) A simplified Finite-Element model of the Tower was put together considering the inclination in the N-S direction, which is potentially important for base bending due to vertical seismic action. The foundation impedance matrix was first evaluated based on

a sensitivity analysis; then a model updating was performed based on the frequency values resulting in very good agreement with the experimental data.

(6) The vertical mode response resulted in a motion in the direction of the inclined axis of the tower (not vertical) and lead to a moderate increase in base bending. Had the specific mode been vertical instead of axial, the increase is base bending over that due to purely horizontal excitation would have exceeded 50%. The number of dynamic sensors mounted on the structure is too low to allow proper identification of the mode shapes, especially torsional ones. Moreover, the existing far field station is located far too close to the Tower not to be influenced by its response. Selecting a new set of measurement points, located sufficiently far from the structure, is essential for a reliable monitoring of the free field motion. Finally, an upgrade in the seismic monitoring system would allow for better data storage and management. Given the strong interest in establishing the static characteristics of the structure from dynamic measurements, further work should be devoted in this direction too.

(7) The shift in natural period due to SSI, from about 0.3s under fixed-base conditions to over 1s considering soil compliance ($\tilde{T}/T \approx 3$) and a corresponding wave parameter ($1/\sigma$) of about 0.3 are the largest known for a building structure of this height. The reduction in spectral acceleration demand due to SSI is on the order of 200-450% depending on the ground motion considered. This reduction is probably a lower bound, as it does not account for period elongation due to non-linear soil response resulting from inertial interaction and associated increase in damping. Evidently, the beneficial effect of SSI on seismic response of the Tower is massive and may explain the lack of earthquake damage on the structure, despite its severe inclination, low strength and limited ductility. Nevertheless, it is fair to mention that the survival of the structure can be partially attributed to the modest seismicity of the area as well.

ACKNOWLEDGEMENTS

The study at hand was funded by Opera della Primaziale Pisana and coordinated by Camillo Nuti. Special thanks are due to Professor Luca Sanpaolesi for his comments and suggestions. Giuseppe Quaranta and Giorgio Monti also acknowledge the support of Sapienza University of Rome through the project “Smart solutions for the assessment of structures in seismic areas”. The authors would also like to thank INGV of Rome (Dr. Giuliano Milana) for providing the

equipment for the two-dimensional geophysical array. The authors also benefitted from discussions with Professors Eduardo Kausel and Carlo Lai.

REFERENCES

Acunzo, G., Pagliaroli, A., Scasserra G., 2014. In-Spector: un software di supporto alla selezione di accelerogrammi naturali spettro-compatibili per analisi geotecniche e strutturali. Proceedings of 33rd conference of GNGTS, Bologna, Italy (in Italian).

Akkar, S. and Bommer J.J., 2010. Empirical equations for the prediction of PGA, PGV, and spectral accelerations in Europe, the Mediterranean region, and the Middle East. *Seismol. Res. Lett.* **81**(2), 195-206.

Alisud S.P.A., 1996. Rilevamento architettonico della Piazza dei Miracoli e della Torre di Pisa, Incarico Prot. n. JAM2660.1/tp. (In Italian).

Angina, A., Steri, A., Stacul, S., Lo Presti, D. (2018). Free-Field Seismic Response Analysis: The Piazza dei Miracoli in Pisa Case Study. *International Journal of Geotechnical Earthquake Engineering (IJGEE)*, **9**(1), 1-21.

Atzeni, C., Bicci, A., Dei, D., Fratini, M. and Pieraccini M., 2010. Remote survey of the leaning tower of Pisa by interferometric sensing. *IEEE Geoscience and Remote Sensing Letters*, **7**(1), 185-189.

Bartelletti, R., Fiorentino, G., Lanzo, G., Lavorato, D., Marano, G.C., Monti, G., Nuti, C., Quaranta, G., Sabetta, F. and Squeglia N., 2016a. Behavior of the Leaning Tower of Pisa: Analysis of Experimental Data from Structural Dynamic Monitoring, *Appl. Mech. Mater.*, **847**, 445-453.

Bartelletti, R., Fiorentino, G., Lanzo, G., Lavorato, D., Marano, G.C., Monti, G., Nuti, C., Quaranta, G., Sabetta, F. and Squeglia N., 2016b. Behavior of the Leaning Tower of Pisa: Insights on Seismic Input and Soil-Structure Interaction, *Appl. Mech. Mater.*, **847**, 454-462.

Bommer, J.J. and Abrahamson N.A., 2006. Why do modern probabilistic seismic-hazard analyses often lead to increased hazard estimates? *Bull. Seismol. Soc. Am.* **96**(6), 1967–1977.

Bommer, J.J. and Acevedo A.B., 2004. The use of real earthquake accelerograms as input to dynamic analysis. *J. Earthq. Eng.* **8**(spec01), 43-91.

Burland, J.B., Jamiolkowski, M., Squeglia, N. and Viggiani C., 2013. The leaning Tower of Pisa. *Geotechnics and Heritage: Case Histories* (ed. Viggiani, C.) CRC Press, 207–227.

Burland, J.B., Jamiolkowski, M. and Viggiani C., 2009. Leaning Tower of Pisa: Behavior after stabilization operations. *International Journal of Geoengineering Case Histories* **3**(1), 156-169.

Capon, J. (1969). High-resolution frequency-wavenumber spectrum analysis. *Proceedings of the IEEE* **57**(8) 1408-1418.

Castellaro, S. and Mulargia F., 2010. How far from a building does the ground-motion free-field start? The cases of three famous towers and a modern building. *B. Seismol. Soc. Am.* **100**(5A), 2080-2094.

CEN (2004) Eurocode 8: design of structures for earthquake resistance. Part 1: general rules, seismic actions and rules for buildings (EN1998-1). CEN, Brussels.

Cestelli Guidi, C., Croce, A., Skempton, A.W., Schultze, E., Calabresi, G. and Viggiani C., 1971. Caratteristiche geotecniche del sottosuolo della Torre. *Ricerche e studi sulla Torre pendente di Pisa ed i fenomeni connessi alle condizioni d'ambiente* **1**, 179-200 (in Italian).

Consorzio Progetto Torre di Pisa (2000), *Esecuzione di prova geofisica Cross Hole nella Piazza del Duomo – Pisa*. Comitato per gli interventi di consolidamento e restauro della Torre di Pisa.

Consorzio Progetto Torre di Pisa (2001), *Ripristino del fondo del Catino e sua connessione con la Torre*. Comitato per gli interventi di consolidamento e restauro della Torre di Pisa. (in Italian).

Cresy, E., and Taylor G.L., 1829. Architecture of the Middle Ages in Italy: Illustrated by views, plans, elevations, sections and details of the cathedral, baptistry, leaning Tower of campanile and Campo Santo at Pisa from drawings and measurements taken in the year 1817. London.

D'Elia, B., Lanzo, G., and Pagliaroli A., 2003. Small-strain stiffness and damping of soils in a direct simple shear device. *Proceedings of the 7th Pacific Conference on Earthquake Engineering*, 13-15 February 2003, Christchurch, New Zealand.

Darendeli, M.B., 2001. Development of a new family of normalized modulus reduction and material damping curves. Ph.D. Thesis, Department of Civil Engineering, University of Texas, Austin.

Desideri A, Russo G, and Viggiani C., 1997. La stabilità di torri su terreno deformabile. *Rivista Italiana di Geotecnica,* 1:5-29 (in Italian).

Fiorentino, G., Nuti, C., Squeglia, N., Lavorato, D., Stacul, S. (2018). One-Dimensional Nonlinear Seismic Response Analysis Using Strength-Controlled Constitutive Models: The Case of the Leaning Tower of Pisa's Subsoil. *Geosciences* **8**(7), 228.

Fiorentino, G., Lavorato, D., Quaranta, G., Pagliaroli, A., Carlucci, G., Mylonakis, G., Squeglia, N., Briseghella, B., Monti, G., Nuti, C., 2017. Leaning Tower of Pisa: recent studies on dynamic response and soil-structure interaction, Paper No. 11588, in Proceedings of the 16th European Conference of Earthquake Engineering (16ECEE), 18-21 June, Thessaloniki, Greece.

Fiorentino, G., Lavorato, D., Quaranta, G., Pagliaroli, A., Carlucci, G., Nuti, C., Sabetta, F., Della Monica, G., Piersanti, M., Lanzo, G., Marano, G.C., Monti, G., Squeglia, N., and Bartelletti R., 2017. Numerical and experimental analysis of the leaning Tower of Pisa under earthquake, *Procedia Engineering* **199**, 3350-3355. https://doi.org/10.1016/j.proeng.2017.09.559.

Givens, M.J., Mylonakis, G. and Stewart J.P., 2016. Modular Analytical Solutions for Foundation Damping in Soil-Structure Interaction Applications. *Earthquake Spectra* **32**(3), 1749-1768.

Grandori, G. and Faccioli E., 1993. *Studio per la definizione del terremoto di verifica per le analisi sulla Torre di Pisa – Relazione finale.* Comitato per gli interventi di consolidamento e restauro della Torre di Pisa. (in Italian).

Grandori, G., Faccioli, E. and Paolucci R., 1999. *Approfondimento degli studi sul problema sismico*. Comitato per gli interventi di consolidamento e restauro della Torre di Pisa. (in Italian).

Hudson, M., Idriss, I.M. and Beikae M., 1994. QUAD4M: a computer program to evaluate the seismic response of soil structures using finite element procedures and incorporating a compliant base. Center for Geotechnical Modeling, Department of Civil and Environmental Engineering, University of California Davis.

Impavido, M., Lancellotta, R., Lo Presti, D. and R. Pallara, 1993. *Esecuzione di prove relative alla caratterizzazione del comportamento meccanico dell'argilla di Pisa. Rapporto di ricerca 2.10, Prove di colonna risonante.* Contratto di ricerca Politecnico di Torino-Consorzio Torre di Pisa.

Istituto Sperimentale Modelli e Strutture, 1992. *Modellazione numerica della struttura della Torre – Calibrazione dello stick model dell'elevazione e analisi a spettro di risposta*. Comitato per gli interventi di consolidamento e restauro della Torre di Pisa. (in Italian).

Karimi, Z., Bullock, Z, Dashti, S., Liel, A., and Porter, K., 2017. Influence of Soil and Structural Parameters on Liquefaction-Induced Settlement of Foundations. *3rd International Conference on Performance-based Design in Earthquake Geotechnical Engineering* (PBD-III), Vancouver, Canada.

Kramer, S. L., Sideras, S.S., and Greenfield, M.W., 2015. The Timing of Liquefaction and Its Utility in Liquefaction Hazard Evaluation, *6th International Conference on Earthquake Geotechnical Engineering*, 13-15 February 2003, Christchurch, New Zealand.

Kottke, A.R., Wang, X. and Rathje E.M., 2013. Technical manual for STRATA. Geotechnical Engineering Center, Dpt. of Civil. Architectural and Environmental Engineering, University of Texas, October 2013.

Lermo, J. and Chávez-García F.J., 1993. Site Effect Evaluation Using Spectral Ratios with only one Station. *Bull. Seismol. Soc. Am.* **83**(5):1574-1594.

Liu, T., Zhang, Q., Zordan, T., and Briseghella B., 2016. Finite Element Model Updating of Canonica Bridge Using Experimental Modal Data and Genetic Algorithm. *Struct. Eng. Int.* **26**(1), 27-36.

Luzi, L., Puglia, R., and Russo E., 2016. Engineering Strong Motion Database, version 1.0. Istituto Nazionale di Geofisica e Vulcanologia, Observatories & Research Facilities for European Seismology. doi: 10.13127/ESM.

Macchi, G. and Ghelfi S., 2005. Problemi di Consolidamento Strutturale in La Torre di Pisa – Gli studi e gli interventi che hanno consentito la stabilizzazione della Torre di Pisa. *Bollettino d'arte*, vol.3.

Marano, G.C., Quaranta, G. and Monti G., 2011. Modified genetic algorithm for the dynamic identification of structural systems using incomplete measurements. *Computer-Aided Civil and Infrastructure Engineering* **26**(2), 92-110.

Maravas, A., Mylonakis, G., and Karabalis, D., 2014. Simplified discrete systems for dynamic analysis of structures on footings and piles, *Soil Dynamics & Earthquake Engineering*, **61**, 29-39.

Margottini, C., Molin, D. and Serva L., 1992. Intensity vs. ground motion: a new approach using Italian data. *Eng. Geol.* **33**(1), 45-58.

Monti, G., Quaranta. and Marano G.C. (2009) Genetic-algorithm-based strategies for dynamic identification of nonlinear systems with noise-corrupted response. *J. Comput. Civil Eng.* **24**(2), 173-187.

Mylonakis, G., Nikolaou, S., and Gazetas G., 2006. Footings under seismic loading: Analysis and design issues with emphasis on bridge foundations. *Soil Dyn. Earthquake Eng.* **26**(9), 824-853.

Nakamura, Y., 1989. *A method for dynamic characteristics estimation of subsurface using microtremor on the ground surface*. Railway Technical Research Institute, Quarterly Reports, **30**(1).

Nakamura, Y. (2000) Clear identification of fundamental idea of Nakamura's technique and its applications. *Proceeding of the 12th WCEE*, 30 January – 4 February, Auckland, New Zealand.

Nakamura, Y., Gurler, E.D. and Saita J., 1999. Dynamic characteristics of leaning tower of Pisa using microtremor – Preliminary results. *Proceedings of the 25th JSCE Earthquake Engineering Symposium*, Tokyo (Japan) **2**, 921-924.

NIST GCR 12-917-21, 2012. *Soil Structure Interaction for Building Structures. NEHRP Consultants Joint Venture. A partnership of the Applied Technology Council and the Consortium of Universities for Research in Earthquake Engineering.*

Opera della Primaziale Pisana, 2015. *Prova con dilatometro sismico* (SDMT) (in Italian).

Ordaz, M., Arboleda, J., and Singh S.K., 1995. A scheme of random summation of an empirical Green's function to estimate ground motions from future large earthquakes. *Bull. Seismol. Soc. Am.* **85**(6), 1635-1647.

Ordaz, M., Martinelli, F., Aguilar, A., Arboleda, J., Meletti, C. and D'Amico V., 2014. *CRISIS 2014 – Program for computing seismic hazard*. Instituto de Ingeniería, UNAM.

Pilla L., 1846.Istoria del tremuoto che ha devastato i paesi della costa toscana il dì 14 agosto 1846, Pisa.

Postpischl, D., Stucchi, M., Bellani A., 1991. Some ideas for a databank of macroseismic data. *Tectonophysics* **193**(1-3), 215-223.

Rampello, S. and Callisto L., 1998. A study on the subsoil of the Tower of Pisa based on results from standard and high-quality samples. *Can. Geotech. J.* **35**(6), 1074-1092.

Rollins, K.M., Evans, M.D., Diehl, N.B. and Daily III W.D., 1998. Shear modulus and damping relationships for gravels. *J. Geotech. Geoenviron.* **124**(5), 396-405.

Rovida, A, Locati, M, Camassi, R, Lolli, B and Gasperini P.(eds.), 2016. CPTI15, the 2015 version of the Parametric Catalogue of Italian Earthquakes. Istituto Nazionale di Geofisica e Vulcanologia.

Sabetta, F., 2014. Seismic hazard and design earthquakes for the central archaeological area of Rome, *Bulletin of Earthquake Engineering* **12**(3), 1307-1317.

Sabetta, F., Lucantoni, A., Bungum, H., and Bommer J.J., 2005. Sensitivity of PSHA results to ground-motion prediction relations and logic-tree weights. *Soil Dyn. Earthq. Eng.* **25**, 317–329.

Sambridge, M., 1999. Geophysical inversion with a neighborhood algorithm-II. Appraising the ensemble. *Geophys. J. Int.* **138**(3), 727-746.

SESAME European research project WP13 – Deliverable D24.13, 2005. *Recommendations for quality array measurements and processing*.

SESAME European research project WP03 – Deliverable D09.03, 2003. *H/V Technique: Data Processing Report on the Multiplatform H/V Processing Software J-SESAME.*

Squeglia, N., Bentivoglio, G., 2015. Role of monitoring in historical building restoration: The case of Leaning Tower of Pisa. *Int. J. Archit. Herit.* **9**(1), 38-47.

Squeglia, N., Stacul, S., & Diddi, E. (2015). The restoration of San Paolo Church in Pisa: geotechnical aspects. *Rivista Italiana di Geotecnica*, *49*(3), 58-69.

Star, L., Tileylioglu, S., Givens, M., Mylonakis, G., Stewart J.P., 2018. Evaluation of Soil-Structure Interaction Effects from System Identification of Structures Subject to Forced Vibration Tests, *Soil Dyn. Earthq. Eng.*, (accepted for publication).

Stewart, J. P., and Fenves G.L., 1998. System identification for evaluating soil–structure interaction effects in buildings from strong motion recordings. *Earthquake Eng. Struct. Dyn.* **27**(8), 869-885.

Stewart, J. P., Seed, R. B., and Fenves G.L., 1999a. Seismic soil-structure interaction in buildings. I: Analytical methods. *J. Geotech. Geoenviron* **125**(1), 26-37.

Stewart, J. P., Seed, R. B., and Fenves G.L., 1999b. Seismic soil-structure interaction in buildings. II: Empirical findings. *J. Geotech. Geoenviron*, **125**(1), 38-48.

Sun, H. and Büyüköztürk, O., 2018. The MIT Green Building benchmark problem for structural health monitoring of tall buildings. *Structural Control and Health Monitoring* **25**(3), e2115.

Tokimatsu, K., 1995. Geotechnical site characterization using surface waves. *Proceedings of the 1st ICEGE* (ed. K. Ishihara), Balkema, Leiden, pp. 1333-1368.

Veletsos, A.S., and Wei, Y.T., 1971. Lateral and rocking vibration of footings. *Journal of the Soil Mechanics and Foundations Division* **97**(9), 1227-1248.

Viggiani, C., and Pepe M.C., 2005. Il sottosuolo della Torre in La Torre di Pisa – Gli studi e gli interventi che hanno consentito la stabilizzazione della Torre di Pisa. *Bollettino d'Arte*, vol.2.

Wathelet, M., Jongmans, D., and Ohrnberger, M., 2004. Surface-wave inversion using a direct search algorithm and its application to ambient vibration measurements. *Near Surf. Geophys.* **2**(4), 211-221.

Yoshida, N., 2015. *Seismic Ground Response Analysis*. Springer. DOI: 10.1007/978-94-017-9460-2